The trans-Turing Machine

Gábor Vattay
Dept. of Physics of Complex Systems, Eötvös University

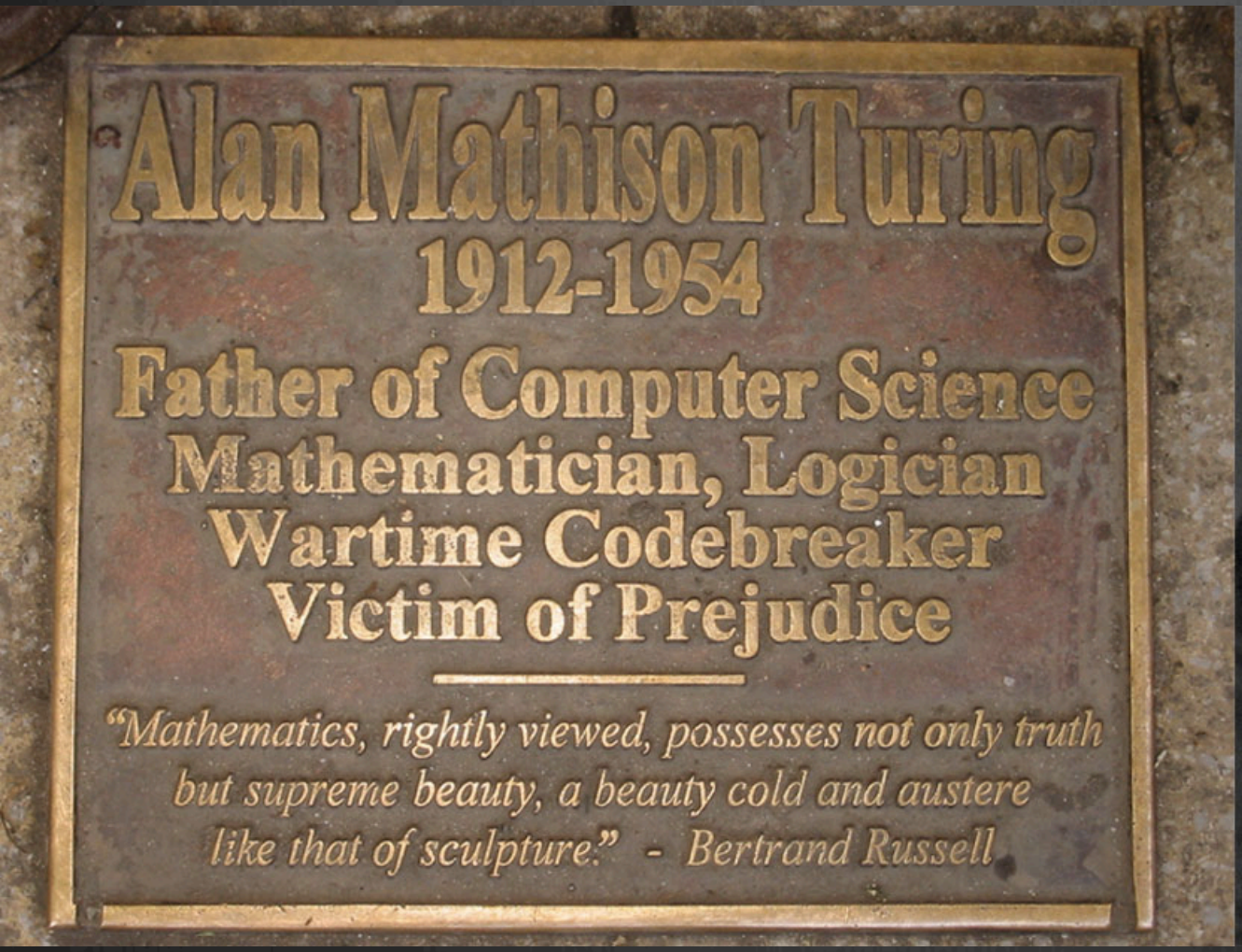
Alan Mathison Turing
1912-1954
Father of Computer Science
Mathematician, Logician
Wartime Codebreaker
Victim of Prejudice
"Mathematics, rightly viewed, possesses not only truth but supreme beauty, a beauty cold and austere like that of sculpture." - Bertrand Russell

Samuel N Alexander

First Draft of a Report
on the EDVAC

by

John von Neumann

Contract No. W-670-ORD-4926

Between the

United States Army Ordnance Department

and the

University of Pennsylvania

Moore School of Electrical Engineering
University of Pennsylvania

June 30, 1945

National Bureau of Standards
Division 12
Data Processing Systems

The Turing Machine

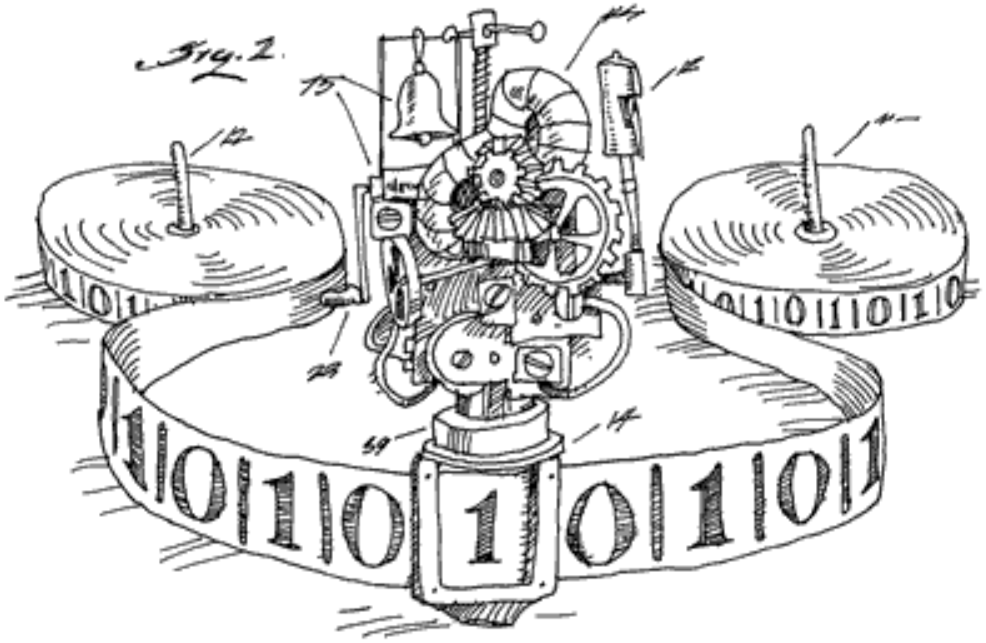

Non-computable numbers, halting problem, Gödel …

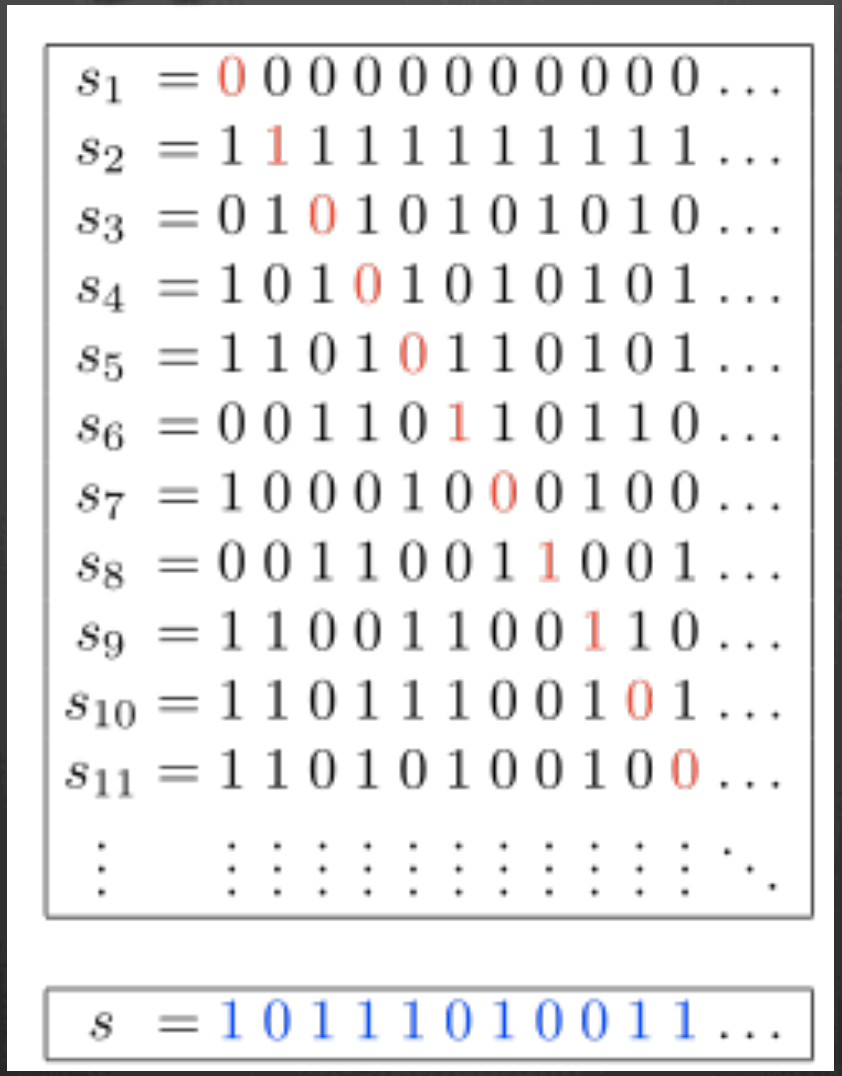

Complexity

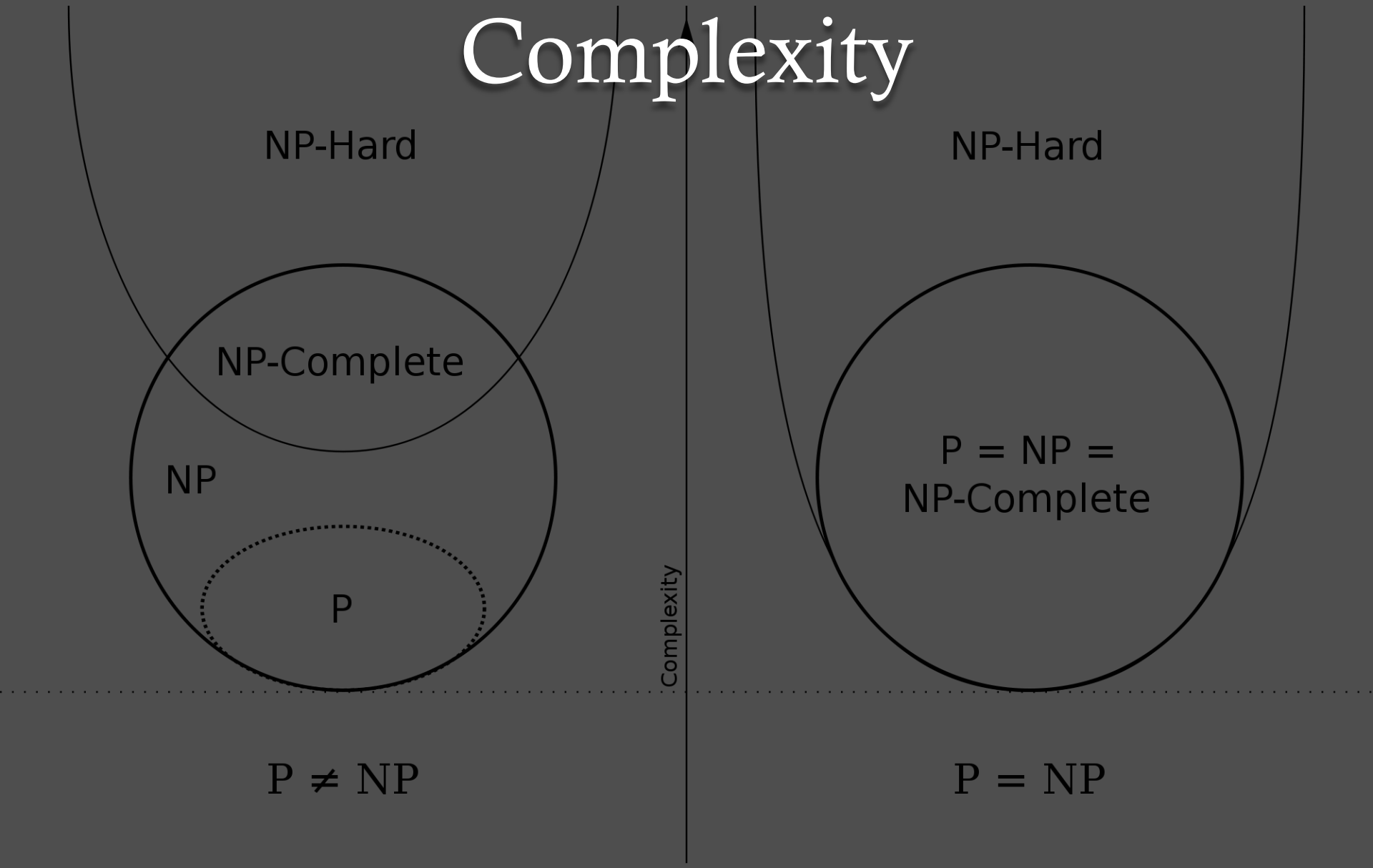
NP-Hard
NP-Complete
NP
P
Complexity
NP-Hard
P = NP =
NP-Complete
P ≠ NP
P = NP

Road trip stopping at major U.S. landmarks

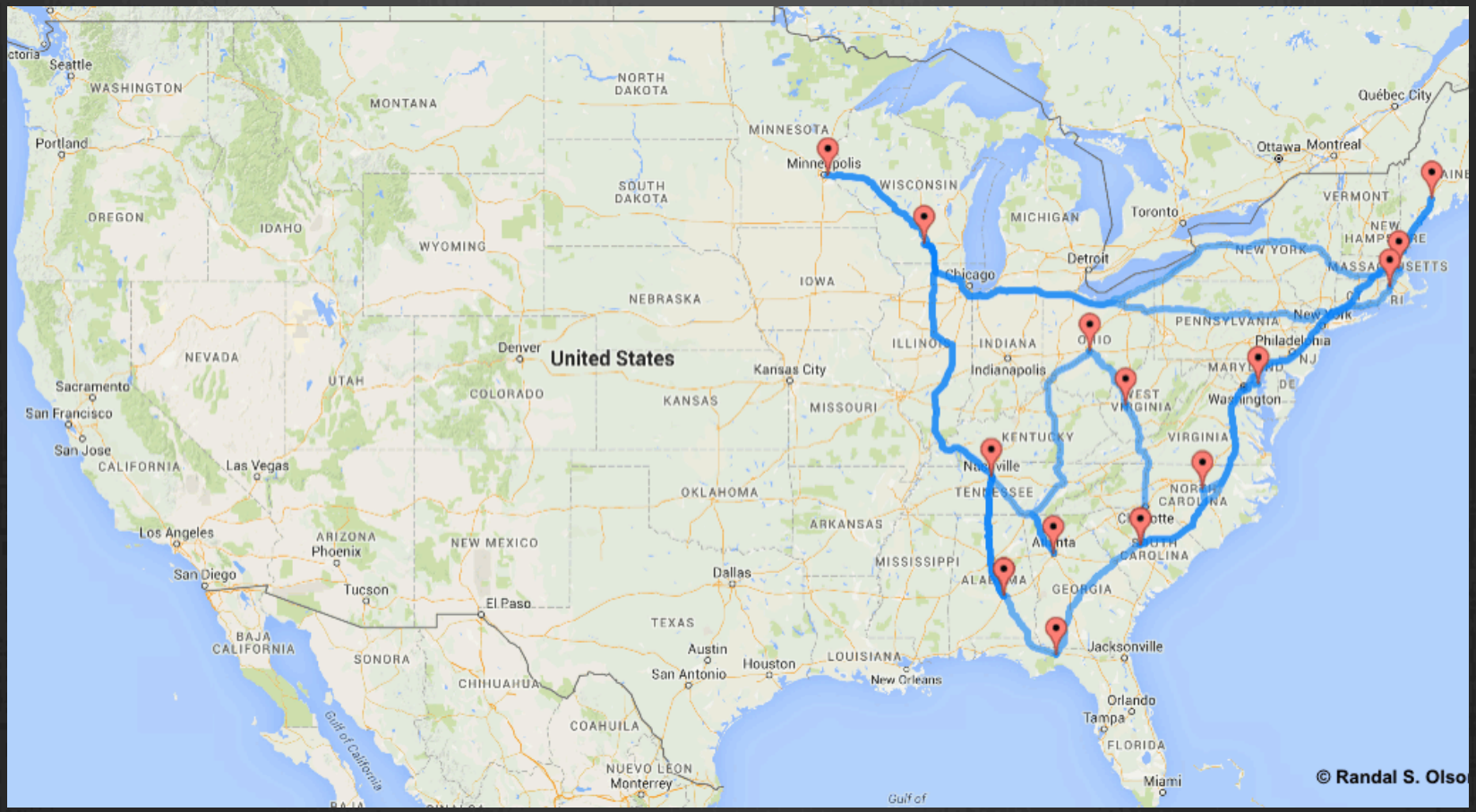

Traveling Salesman Problem

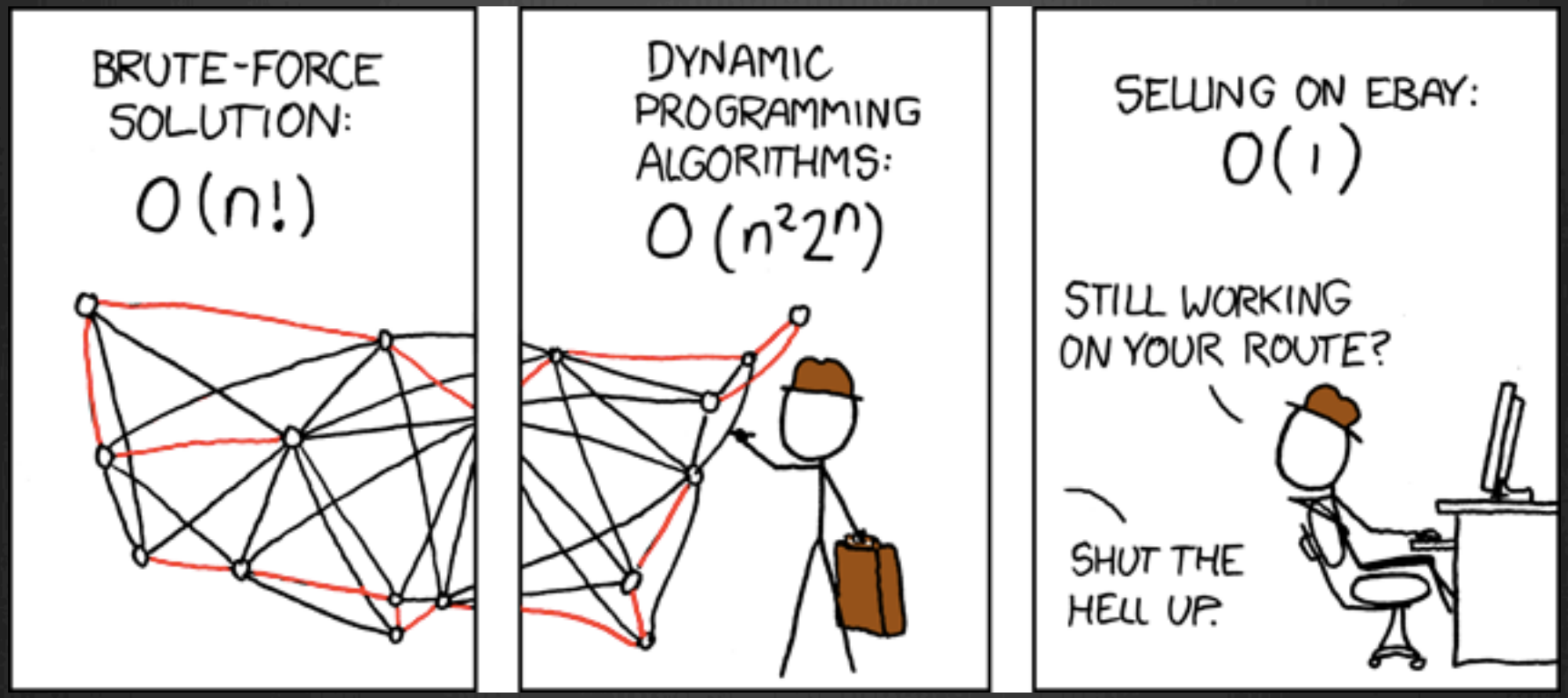

TSP

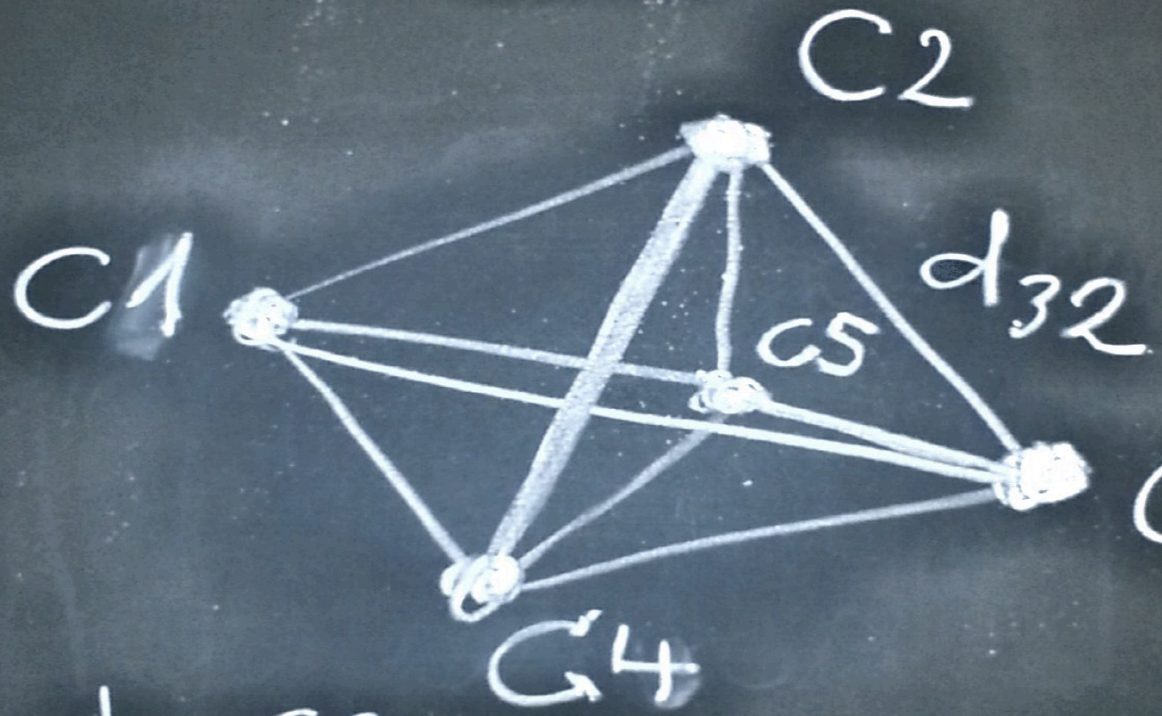

	C2	...
C3	d_{32}	
⋮		

$$W_{32} = d_{32}$$

v \ i	1	2	3	4	5
C1	∅	1	∅	∅	∅
C2	1	∅	∅	∅	∅
C3	∅	∅	∅	1	∅
C4	∅	∅	1	∅	∅
C5	∅	∅	∅	∅	1

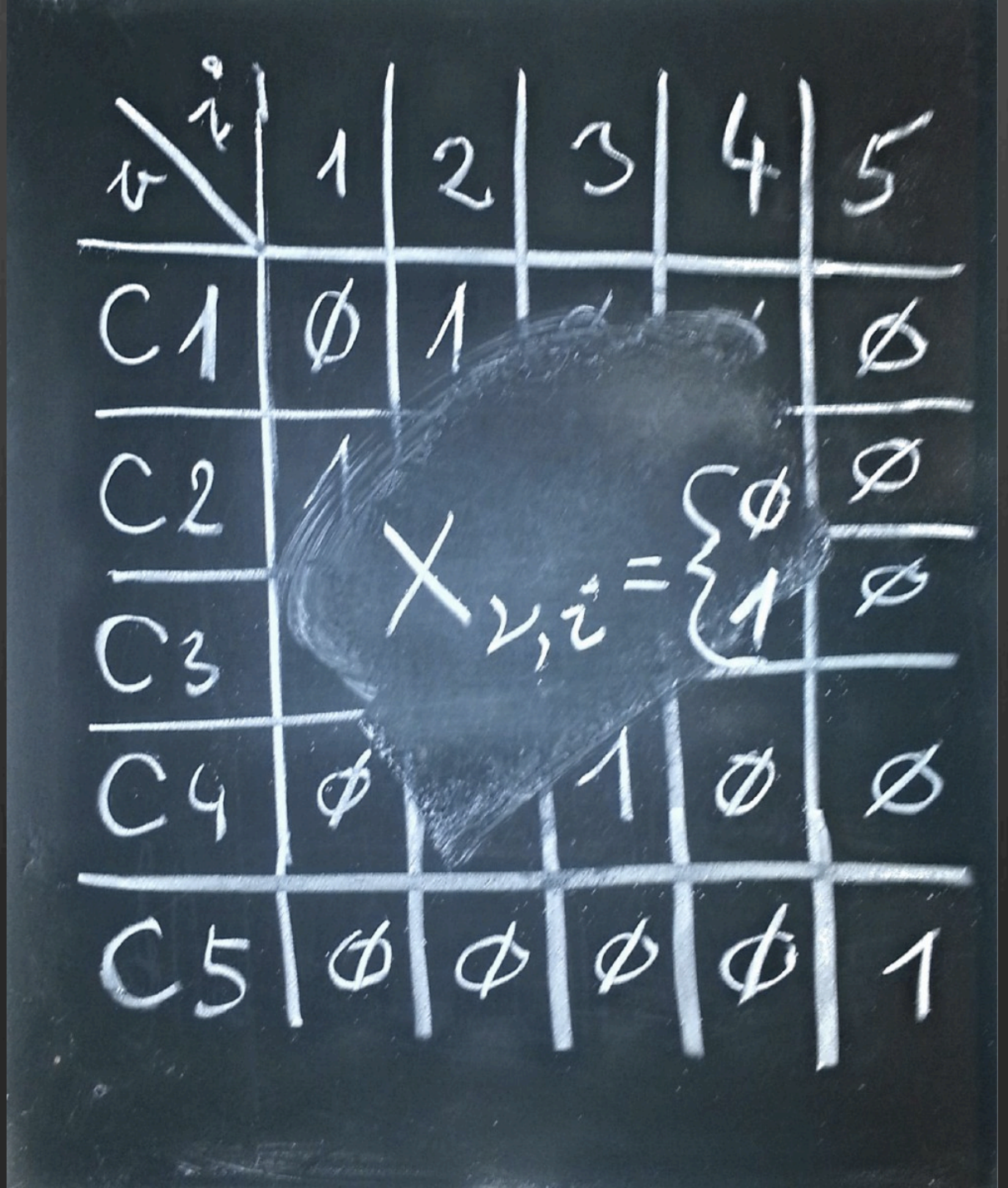
v
i
1
2
3
4
5
C1
C2
C3
C4
C5
$X_{v,i} = \begin{cases} 0 \\ 1 \end{cases}$

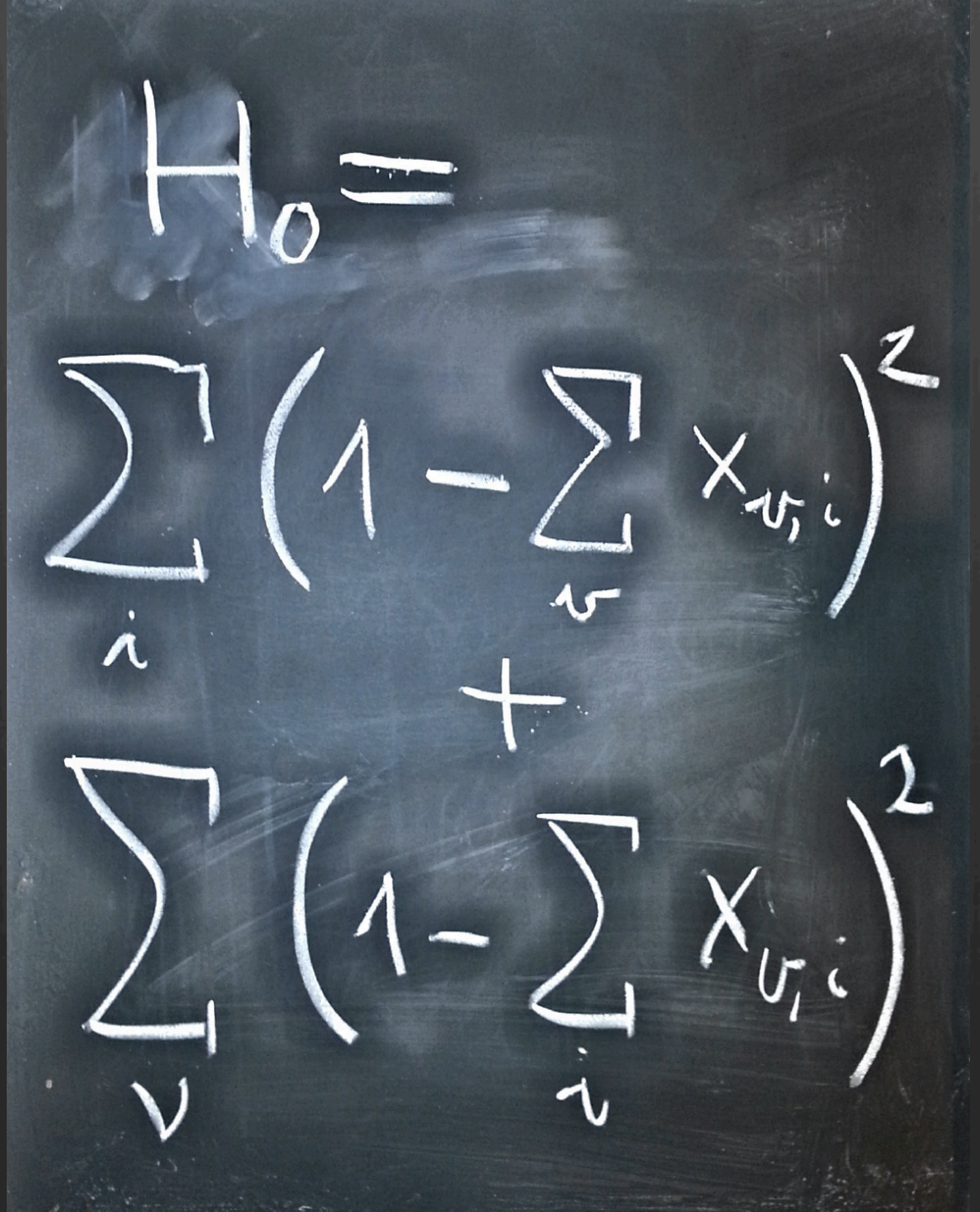
$H_0 =$
$\sum_i \left(1 - \sum_\nu x_{\nu,i}\right)^2$
$+$
$\sum_\nu \left(1 - \sum_i x_{\nu,i}\right)^2$

$$H_1 =$$

$$\sum_{(u,v) \in E} \sum_{i} W_{u,v} X_{u,i} \cdot X_{v,i+1}$$

$$H = H_0 + H_1$$

$$\min_{\{\underline{\underline{x}}\}} H(\underline{\underline{x}})$$

$$\underline{\underline{x}} = ?$$

Optimization!

Simulated annealing

Optimization by Simulated Annealing

S. Kirkpatrick, C. D. Gelatt, Jr., M. P. Vecchi

Summary. There is a deep and useful connection between statistical mechanics (the behavior of systems with many degrees of freedom in thermal equilibrium at a finite temperature) and multivariate or combinatorial optimization (finding the minimum of a given function depending on many parameters). A detailed analogy with annealing in solids provides a framework for optimization of the properties of very large and complex systems. This connection to statistical mechanics exposes new information and provides an unfamiliar perspective on traditional optimization problems and methods.

In this article we briefly review the central constructs in combinatorial optimization and in statistical mechanics and then develop the similarities between the two fields. We show how the Metropolis algorithm for approximate numerical simulation of the behavior of a many-body system at a finite temperature provides a natural tool for bringing the techniques of statistical mechanics to bear on optimization.

We have applied this point of view to a number of problems arising in optimal design of computers. Applications to partitioning, component placement, and wiring of electronic systems are described in this article. In each context, we introduce the problem and discuss

sure of the "goodness" of some complex system. The cost function depends on the detailed configuration of the many parts of that system. We are most familiar with optimization problems occurring in the physical design of computers, so examples used below are drawn from

with N, so that in practice exact solutions can be attempted only on problems involving a few hundred cities or less. The traveling salesman belongs to the large class of NP-complete (nondeterministic polynomial time complete) problems, which has received extensive study in the past 10 years (*3*). No method for exact solution with a computing effort bounded by a power of N has been found for any of these problems, but if such a solution were found, it could be mapped into a procedure for solving all members of the class. It is not known what features of the individual problems in the NP-complete class are the cause of their difficulty.

Since the NP-complete class of problems contains many situations of practical interest, heuristic methods have been developed with computational require-

ded from www.sciencemag.org on May 27, 2012

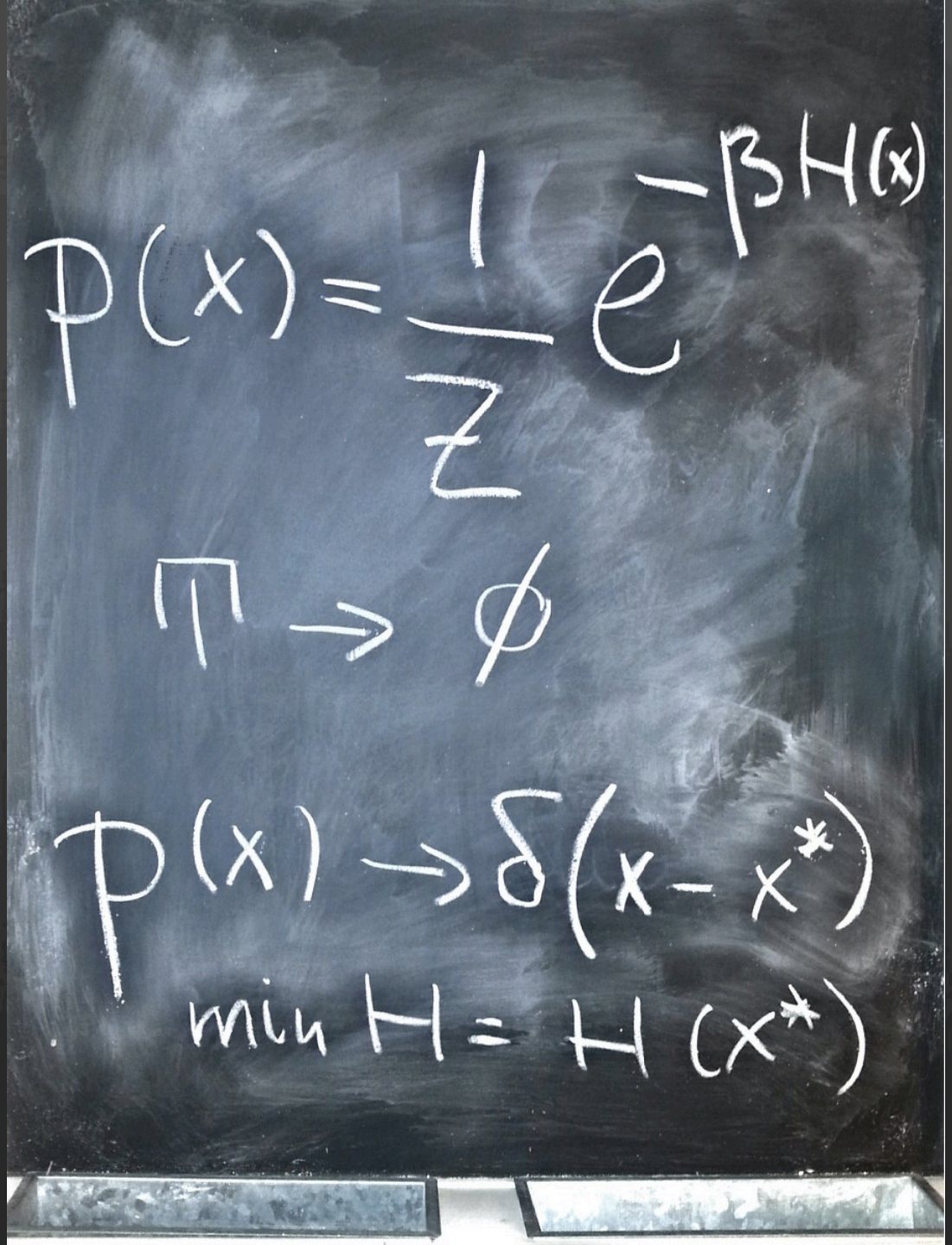
$p(x) = \frac{1}{Z} e^{-\beta H(x)}$
$T \to \phi$
$p(x) \to \delta(x - x^*)$
$\min H = H(x^*)$

Metropolis:

$H(s_1 \ldots\ldots s_N)$

Pick random s_k

flip $s_k \rightarrow -s_k$

accept if $\Delta E < 0$

or with $p = \frac{1}{1 + e^{\beta \Delta E}}$

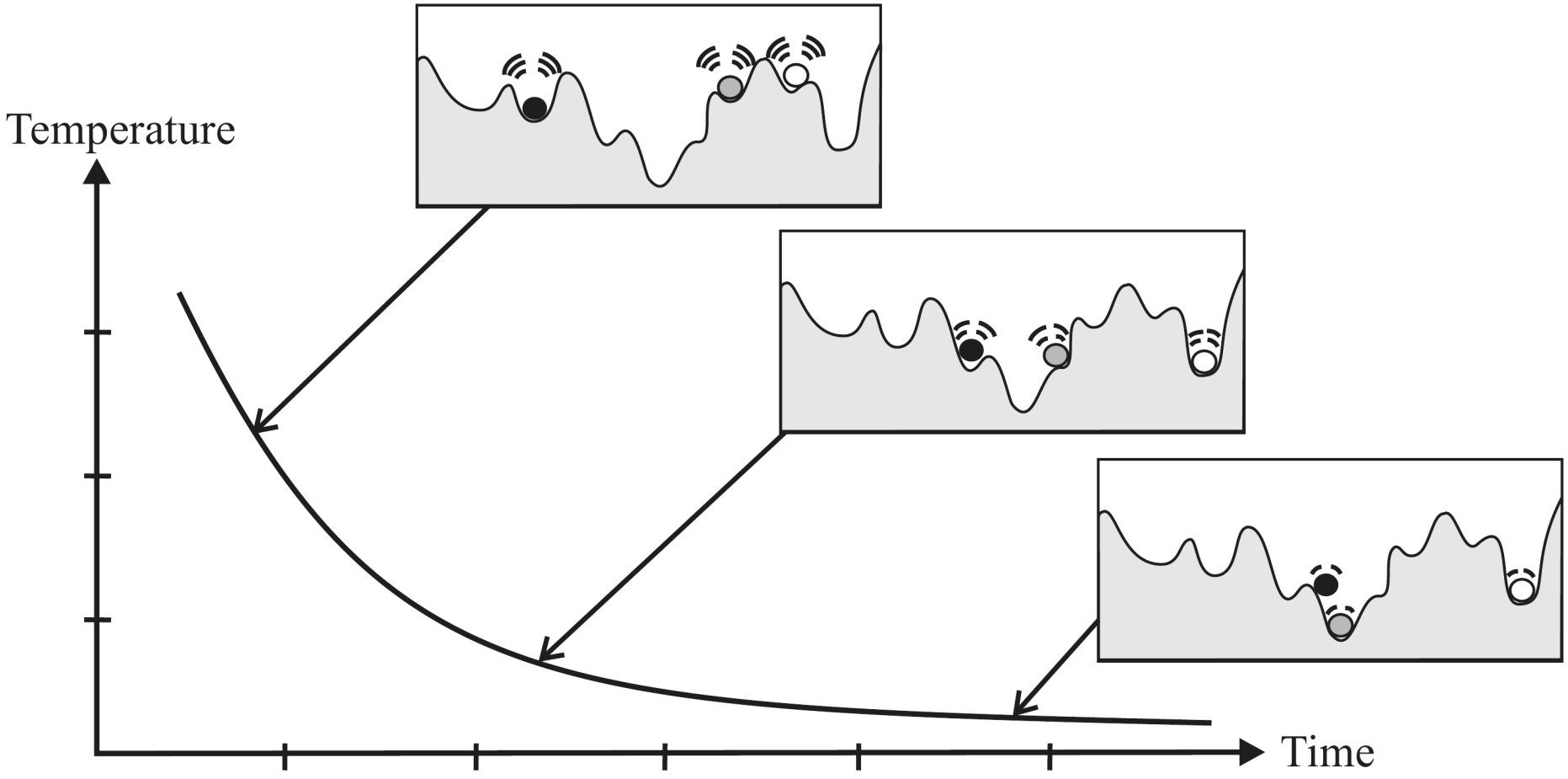
Temperature
Time

Computational complexity 2.0

- Number of steps a TM takes to solve the problem
- Number of steps a TM takes to solve the problem in the worst case
- Average time needed to solve a probable instance of the problem
- Computational problems become statistical physical problems
- Worst case scenario is astronomically improbable in the thermodynamic limit (infinit number of cities)
- Simulated annealing is the best heuristic method as of today

Adiabatic Quantum Computation

Quantum Computation by Adiabatic Evolution

Edward Farhi, Jeffrey Goldstone*
Center for Theoretical Physics
Massachusetts Institute of Technology
Cambridge, MA 02139

Sam Gutmann†
Department of Mathematics
Northeastern University
Boston, MA 02115

Michael Sipser‡
Department of Mathematics
Massachusetts Institute of Technology
Cambridge, MA 02139

MIT CTP # 2936 quant-ph/0001106

quant-ph/0001106v1 28 Jan 2000

Abstract

We give a quantum algorithm for solving instances of the satisfiability problem, based on adiabatic evolution. The evolution of the quantum state is governed by a time-dependent Hamiltonian that interpolates between an initial Hamiltonian, whose ground state is easy to construct, and a final Hamiltonian, whose ground state encodes the satisfying assignment. To ensure that the system evolves to the desired final ground state, the evolution time must be big enough. The time required depends on the minimum energy difference between the two lowest states of the interpolating Hamiltonian. We are unable to estimate this gap in general. We give some special symmetric cases of the satisfiability problem where the symmetry allows us to estimate the gap and we show that, in these cases, our algorithm runs in polynomial time.

Adiabatic theorem

$$i\hbar \frac{\partial \Psi}{\partial t} = H(t)\Psi$$

$$H(t)\psi_k(t) = E_k(t)\psi_k(t)$$

$$\Psi = \sum_k C_k(t)\psi_k(t)\exp\left[-\frac{i}{\hbar}\int_{t_0}^{t} E_k(t')dt'\right]$$

$$\dot{C}_b(t) = -\sum_k C_k(t)\exp\left\{\frac{i}{\hbar}\int_{t_0}^{t}[E_b(t') - E_k(t')]dt'\right\}\left\langle \psi_b \middle| \frac{\partial \psi_k}{\partial t}\right\rangle.$$

$$\left\langle \frac{\partial \psi_k}{\partial t} \middle| \psi_k \right\rangle + \left\langle \psi_k \middle| \frac{\partial \psi_k}{\partial t} \right\rangle = \alpha_k^*(t) + \alpha_k(t) = 0$$

$$\alpha_b(t) = \langle \psi_b | \partial \psi_b / \partial t \rangle = \mathrm{i}\beta_b(t)$$

$$C_k'(t) = C_k(t) \exp\left[\mathrm{i} \int_{t_0}^{t} \beta_k(t') \mathrm{d}t' \right]$$

$$\dot{C}_b(t) = \sum_{k \neq b} \frac{C_k(t)}{\hbar \omega_{bk}(t)} \left(\frac{\partial H}{\partial t} \right)_{bk} \exp\left[\mathrm{i} \int_{t_0}^{t} \omega_{bk}(t') \mathrm{d}t' \right]$$

$$\omega_{bk}(t) = \frac{E_b(t) - E_k(t)}{\hbar}, \quad b \neq k.$$

$$C_k = \delta_{ka}$$

$$C_b(t) = \hbar^{-1} \int_{t_0}^{t} \mathrm{d}t' \omega_{ba}^{-1}(t') \left(\frac{\partial H(t')}{\partial t'} \right)_{ba} \exp\left[\mathrm{i} \int_{t_0}^{t'} \omega_{ba}(t'') \mathrm{d}t'' \right],$$

$$C_b(t) \simeq (\mathrm{i}\hbar)^{-1} \omega_{ba}^{-2} \left(\frac{\partial H}{\partial t} \right)_{ba} \{\exp[\mathrm{i}\omega_{ba}(t - t_0)] - 1\}$$

$$H = \left(1 - \frac{t}{T_A}\right) H_0 + \frac{t}{T_A} H_1$$

$$\frac{\partial H}{\partial t} = -\frac{1}{T_A}(H_0 - H_1)$$

$$C_1(t) \approx \frac{1}{i\hbar} \frac{1}{(E_0 - E_1)^2} \frac{1}{T_A} \langle 0 | H_0 - H_1 | 1 \rangle \left\{ e^{\frac{i}{\hbar}(E_1 - E_0)T} - 1 \right\}$$

Gap $\longrightarrow \Delta$; Annealing time $\longleftarrow$

$$T_A >> \frac{\max |\langle 0 | H_0 - H_1 | 1 \rangle|}{\min \Delta^2 \hbar}$$

System stays in ground state all the time!

$$T = \mathrm{O}\left[\exp\left(\alpha N^{\beta}\right)\right]$$

$$\sigma_z \begin{pmatrix} 1 \\ 0 \end{pmatrix} = \begin{pmatrix} 1 \\ 0 \end{pmatrix} \Rightarrow \quad \sigma_z |s\rangle = s|s\rangle$$

$$\sigma_z \begin{pmatrix} 0 \\ 1 \end{pmatrix} = \begin{pmatrix} 0 \\ -1 \end{pmatrix}$$

$$\sigma_x \begin{pmatrix} 0 \\ 1 \end{pmatrix} = \begin{pmatrix} 1 \\ 0 \end{pmatrix} \Rightarrow \quad \sigma_x |s\rangle = |-s\rangle$$

$$\sigma_x \begin{pmatrix} 1 \\ 0 \end{pmatrix} = \begin{pmatrix} 0 \\ 1 \end{pmatrix}$$

$$\sigma_x \frac{1}{\sqrt{2}}(|s\rangle + |-s\rangle) = \frac{1}{\sqrt{2}}(|s\rangle + |-s\rangle)$$

$$\sigma_x \frac{1}{\sqrt{2}}(|s\rangle - |-s\rangle) = \frac{1}{\sqrt{2}}(+|-s\rangle - |s\rangle) =$$

$$= -\frac{1}{\sqrt{2}}(|s\rangle - |-s\rangle)$$

$$H_0 = -h_0 \sum_{i=1}^{N} \sigma_i^x$$

$$\Psi_0 = \frac{1}{\sqrt{2}} \left(|s_1\rangle + |-s_1\rangle \right) \times \frac{1}{\sqrt{2}} \left(|s_2\rangle + |-s_2\rangle \right) \times \dots$$

$$H_0 \Psi_0 = -h_0 \left(\sum_{i=1}^{N} +1 \right) = -h_0 N \leftarrow \text{Ground state}$$

$$\Psi(x_1, \dots x_N) = \frac{1}{\sqrt{2}} \left(|s_1\rangle + x_1 |-s_1\rangle \right) \times \frac{1}{\sqrt{2}} \left(|s_2\rangle + x_2 |-s_2\rangle \right) \times \dots$$

$$H_0 \Psi = -h_0 \sum_{i=1}^{N} x_i = -h_0 \ell \qquad \ell = -N, \dots \dots + N$$

↑ Excited states

$$\Psi_0 = \frac{1}{2^{N/2}} \sum_{\{s\}} |s_1 s_2 \dots s_N\rangle$$

$$H_1 = -\sum_{i=1}^{N} h_i \sigma_i^z - \sum_{i<j} J_{ij} \sigma_i^z \sigma_j^z$$

$$H_1 |S_1 S_2 \dots S_N\rangle = \left[-\sum_{i=1}^{N} h_i S_i - \sum_{i<j} J_{ij} S_i S_j \right] |S_1 S_2 \dots S_N\rangle$$

Eigenvector!

Eigenvalue!

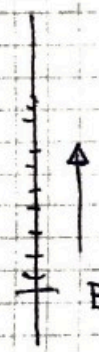

$$E_0 = \min_{\{S\}} \left\{ -\sum_i h_i S_i - \sum_{i<j} J_{ij} S_i S_j \right\} =$$

$$= \left\{ -\sum_i h_i S_i^* - \sum_{ij} J_{ij} S_i^* S_j^* \right\}$$

Ground state: $|S_1^* S_2^* \dots S_N^*\rangle$

is the solution of the Optimization problem!

D-Wave

The Most Advanced Quantum Computer in the World

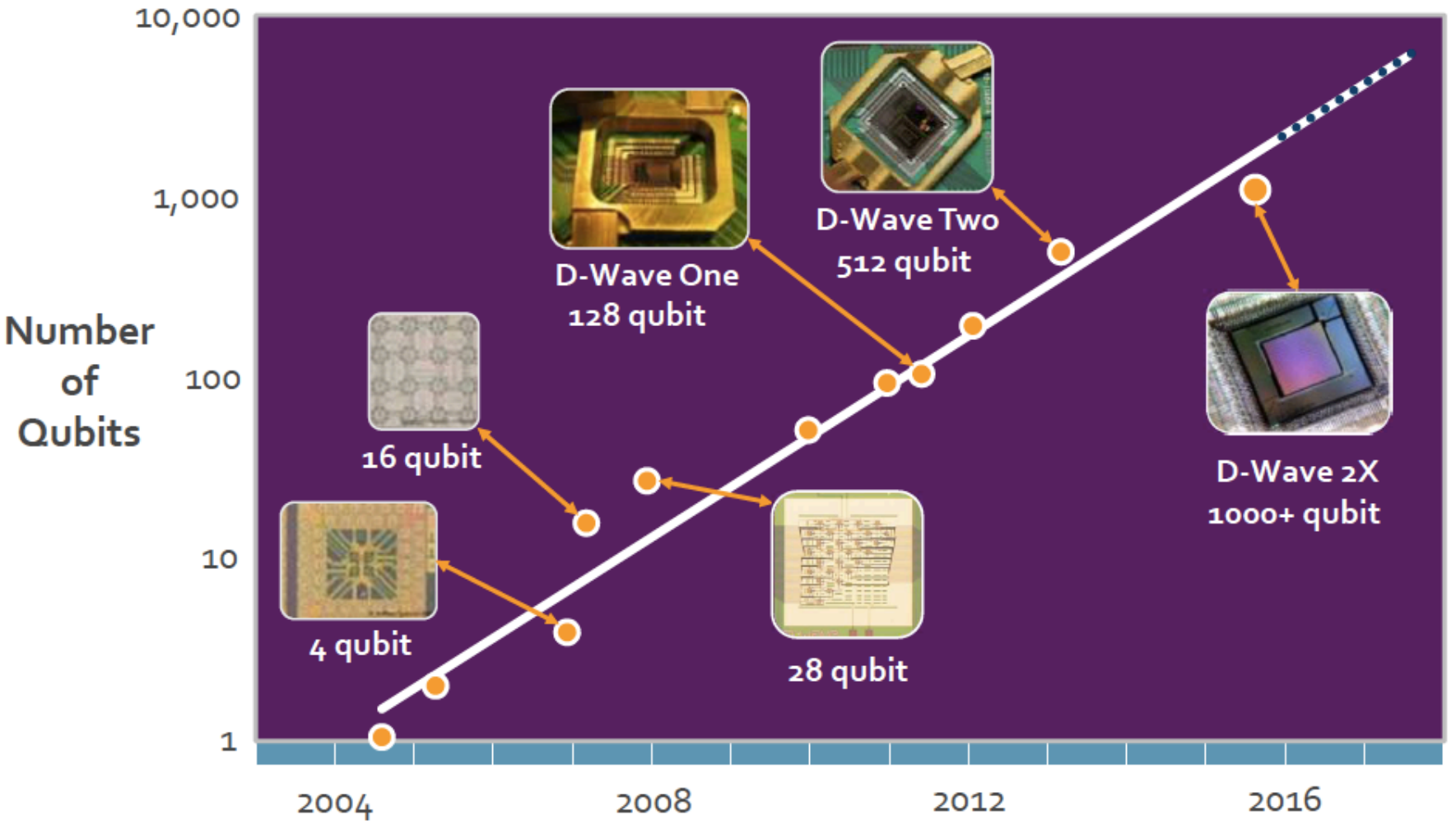

D-Wave
The Quantum Computing Company™

© 2016 D-Wave Systems Inc. All Rights Reserved |

arXiv:0907.3757v2 [quant-ph] 24 Mar 2010

A scalable control system for a superconducting adiabatic quantum optimization processor

M. W. Johnson,[1] P. Bunyk,[1] F. Maibaum,[2] E. Tolkacheva,[1] A. J. Berkley,[1] E. M. Chapple,[1] R. Harris,[1] J. Johansson,[1] T. Lanting,[1] I. Perminov,[1] E. Ladizinsky,[1] T. Oh,[1] and G. Rose[1]

[1] *D-Wave Systems Inc., 100-4401 Still Creek Dr., Burnaby, BC V5C 6G9 Canada* *

[2] *Physikalisch Technische Bundesanstalt, Bundesallee 100, 38116 Braunschweig, Germany*

We have designed, fabricated and operated a scalable system for applying independently programmable time-independent, and limited time-dependent flux biases to control superconducting devices in an integrated circuit. Here we report on the operation of a system designed to supply 64 flux biases to devices in a circuit designed to be a unit cell for a superconducting adiabatic quantum optimization (AQO) system. The system requires six digital address lines, two power lines, and a handful of global analog lines.

PACS numbers: 85.25.Dq, 85.25.Hv, 03.67.Lx

I. INTRODUCTION

Several proposals for how one might implement a quantum computer now exist. One of these is based on enabling adiabatic quantum optimization algorithms in networks of superconducting flux qubits connected via tunable coupling devices [1]. Flux qubits can be manipulated by applying magnetic flux via currents along inductively coupled control lines. This can be accomplished with one analog control line per device driven by room temperature current sources and routed, through appropriate filtering, down to the target device on chip.

Beyond the scale of a few dozens of such qubits the *one-analog-line-per-device* approach becomes impractical. Hundreds of qubits could require thousands of wires, each subject to filtering, cross-talk, and thermal requirements so as to minimize disturbance of the thermal and electromagnetic environment of the targeted qubits, which are operated at milliKelvin temperatures. We require an approach that does not use so many wires.

One advantage of using superconductor based qubits is the existence of a compatible classical digital and mixed signal electronics technology based on the manipulation of single flux quanta (SFQ) [2, 3]. The ability to manufacture classical control circuitry [4–6] on the same chip, with the same fabrication technology as is used in construction of the qubits, addresses many of the thermal and electromagnetic compatibility requirements faced in integrating control circuitry with such a processor. The idea of using SFQ circuitry to control flux qubits is not new, and has investigated by a number of researchers [7–13].

We present here a description of a functioning system of on-chip Programmable Magnetic Memory (PMM) designed to manipulate the parameters and state of superconducting flux qubits and tunable couplers, in such a way as to overcome the scalability limitations of the *one-analog-line-per-device* paradigm. This system comprises three key parts.

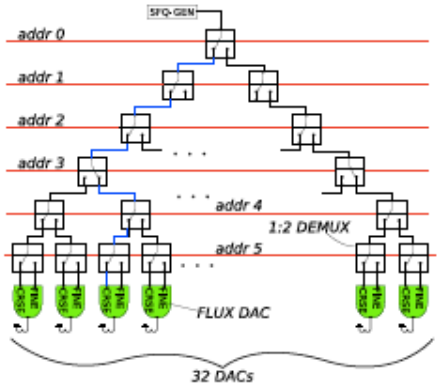

FIG. 1. A 1:32 demultiplexer tree terminating in two-stage multiple flux quantum DACs. The last address selects between the COARSE and FINE stages within a DAC. Two such trees were implemented for the 64 DAC circuit reported here.

The first of these is a SFQ demultiplexer used as an addressing system. It is constructed as a binary tree of $2^N - 1$ 1:2 SFQ demultiplexer gates as shown in Fig. 1. For the specific design discussed here, the number of address lines N is 6. This demultiplexer allows many devices to be addressed using only a few address lines.

The second part is a set of digital-to-analog converters (DACs), located at the leaves of the address tree. These DACs comprise storage inductors that can hold an integer number of single magnetic flux quanta ($\Phi_0 = h/2e$). Their digital input are single flux quanta, and their analog output are the stored flux, which can be coupled into a target device. The magnitude of this output flux is proportional to the number of stored flux quanta. Each

* mwjohnson@dwavesys.com

LETTER

doi:10.1038/nature10012

Quantum annealing with manufactured spins

M. W. Johnson[1], M. H. S. Amin[1], S. Gildert[1], T. Lanting[1], F. Hamze[1], N. Dickson[1], R. Harris[1], A. J. Berkley[1], J. Johansson[2], P. Bunyk[1], E. M. Chapple[1], C. Enderud[1], J. P. Hilton[1], K. Karimi[1], E. Ladizinsky[1], N. Ladizinsky[1], T. Oh[1], I. Perminov[1], C. Rich[1], M. C. Thom[1], E. Tolkacheva[1], C. J. S. Truncik[3], S. Uchaikin[1], J. Wang[1], B. Wilson[1] & G. Rose[1]

Many interesting but practically intractable problems can be reduced to that of finding the ground state of a system of interacting spins; however, finding such a ground state remains computationally difficult[1]. It is believed that the ground state of some naturally occurring spin systems can be effectively attained through a process called quantum annealing[2,3]. If it could be harnessed, quantum annealing might improve on known methods for solving certain types of problem[4,5]. However, physical investigation of quantum annealing has been largely confined to microscopic spins in condensed-matter systems[6–12]. Here we use quantum annealing to find the ground state of an artificial Ising spin system comprising an array of eight superconducting flux quantum bits with programmable spin–spin couplings. We observe a clear signature of quantum annealing, distinguishable from classical thermal annealing through the temperature dependence of the time at which the system dynamics freezes. Our implementation can be configured *in situ* to realize a wide variety of different spin networks, each of which can be monitored as it moves towards a low-energy configuration[13,14]. This programmable artificial spin network bridges the gap between the theoretical study of ideal isolated spin networks and the experimental investigation of bulk magnetic samples. Moreover, with an increased number of spins, such a system may provide a practical physical means to implement a quantum algorithm, possibly allowing more-effective approaches to solving certain classes of hard combinatorial optimization problems.

Physically interesting in their own right, systems of interacting spins also have practical importance for quantum computation[15]. One widely studied example is the Ising spin model, where spins may take on one of two possible values: up or down along a preferred axis. Many seemingly unrelated yet important hard problems, in fields ranging from artificial intelligence[16] to zoology[17], can be reformulated as the problem of finding the lowest energy configuration, or ground state, of an Ising spin system.

Quantum annealing has been proposed as an effective way for finding such a ground state[2–5]. To implement a processor that uses quantum annealing to help solve difficult problems, we would need a programmable quantum spin system in which we could control individual spins and their couplings, perform quantum annealing and then determine the state of each spin. Until recently, physical investigation of quantum annealing has been confined to configurations achievable in condensed-matter systems, such as molecular nanomagnets[6–10] or bulk solids with quantum critical behaviour[11,12]. Unfortunately, these systems cannot be controlled or measured at the level of individual spins, and are typically investigated through the measurement of bulk properties. They are not programmable. Nuclear magnetic resonance techniques have been used to demonstrate a quantum annealing algorithm on three quantum spins[18]. Recently, three trapped ions were used to perform a quantum simulation of a small, frustrated Ising spin system[19].

One possible implementation of an artificial Ising spin system involves superconducting flux quantum bits[20–28] (qubits). We have implemented such a spin system, interconnected as a bipartite graph, using an *in situ* reconfigurable array of coupled superconducting flux qubits[14]. The device fabrication is discussed in Methods and in Supplementary Information. The simplified schematic in Fig. 1a shows two superconducting loops in the qubit, each subject to an external flux bias Φ_{1x} or Φ_{2x}, respectively. The device dynamics can be modelled as a quantum mechanical double-well potential with respect to the flux, Φ_1, in loop 1 (Fig. 1b). The barrier height, δU, is controlled by Φ_{2x}. The energy difference between the two minima, $2h$, is controlled by Φ_{1x}. The two lowest energy states of the system, corresponding to clockwise or anticlockwise circulating current in loop 1, are labelled $|\downarrow\rangle$ and $|\uparrow\rangle$, with flux localized in the left- or the right-hand well (Fig. 1b), respectively. If we consider only these two states (a valid restriction at low temperature), the qubit dynamics is equivalent to those of an Ising spin, and we treat the qubits as such in what follows. Qubits (spins) are

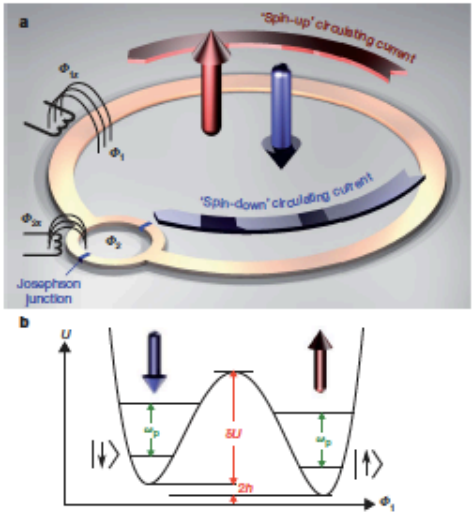

Figure 1 | Superconducting flux qubit. a, Simplified schematic of a superconducting flux qubit acting as a quantum mechanical spin. Circulating current in the qubit loop gives rise to a flux inside, encoding two distinct spin states that can exist in a superposition. **b**, Double-well potential energy diagram and the lowest quantum energy levels corresponding to the qubit. States $|\uparrow\rangle$ and $|\downarrow\rangle$ are the lowest two levels, respectively. The intra-well energy spacing is ω_p. The measurement detects magnetization, and does not distinguish between, say, $|\uparrow\rangle$ and excited states within the right-hand well. In practice, these excitations are exceedingly improbable at the time the state is measured.

[1]D-Wave Systems Inc., 100-4401 Still Creek Drive, Burnaby, British Columbia V5C 6G9, Canada. [2]Department of Natural Sciences, University of Agder, Post Box 422, NO-4604 Kristiansand, Norway. [3]Department of Physics, Simon Fraser University, Burnaby, British Columbia V5A 1S6, Canada.

©2011 Macmillan Publishers Limited. All rights reserved

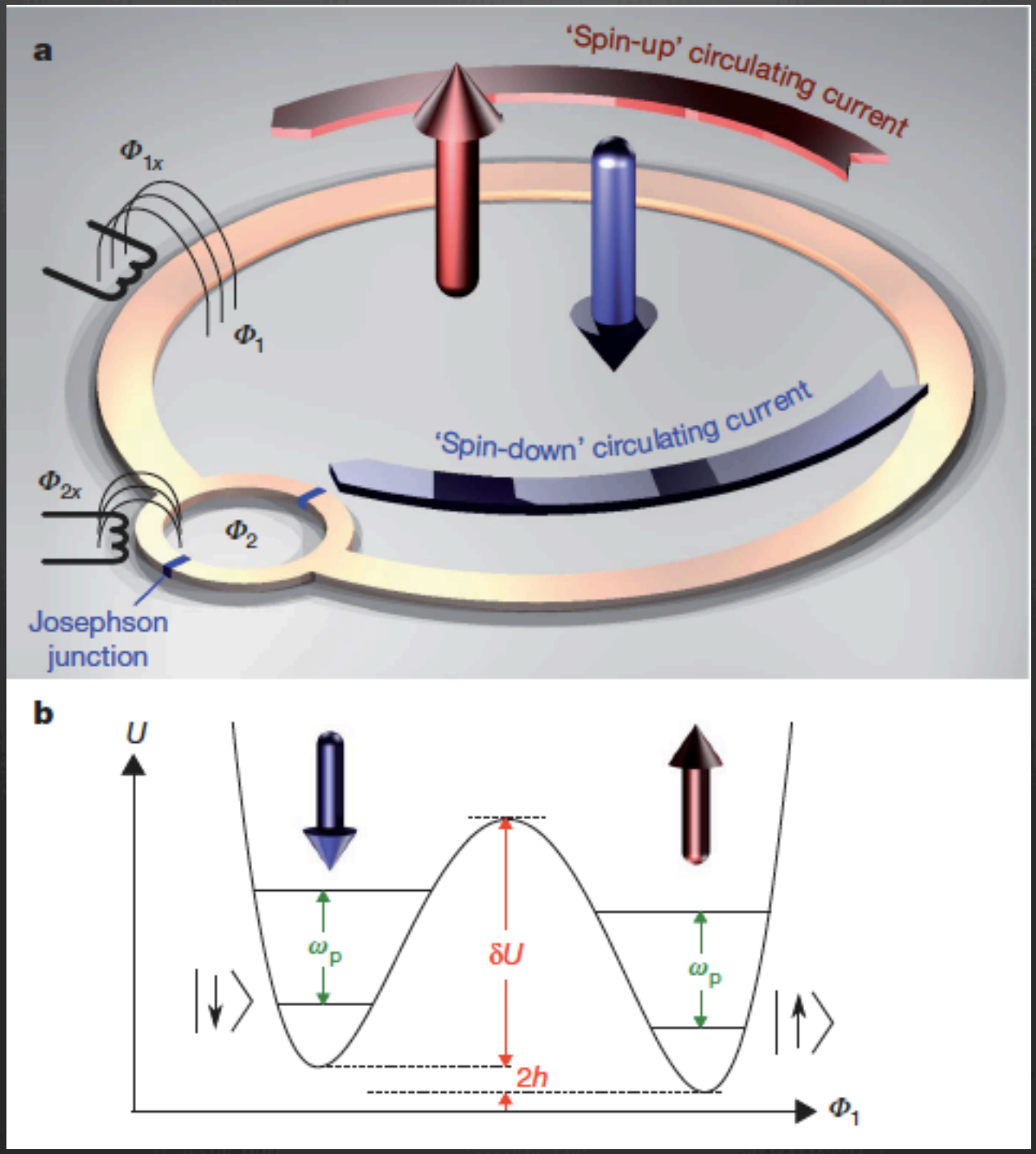
a
'Spin-up' circulating current
Φ_{1x}
Φ_1
'Spin-down' circulating current
Φ_{2x}
Φ_2
Josephson junction
b
U
ω_p
δU
ω_p
2h
Φ_1

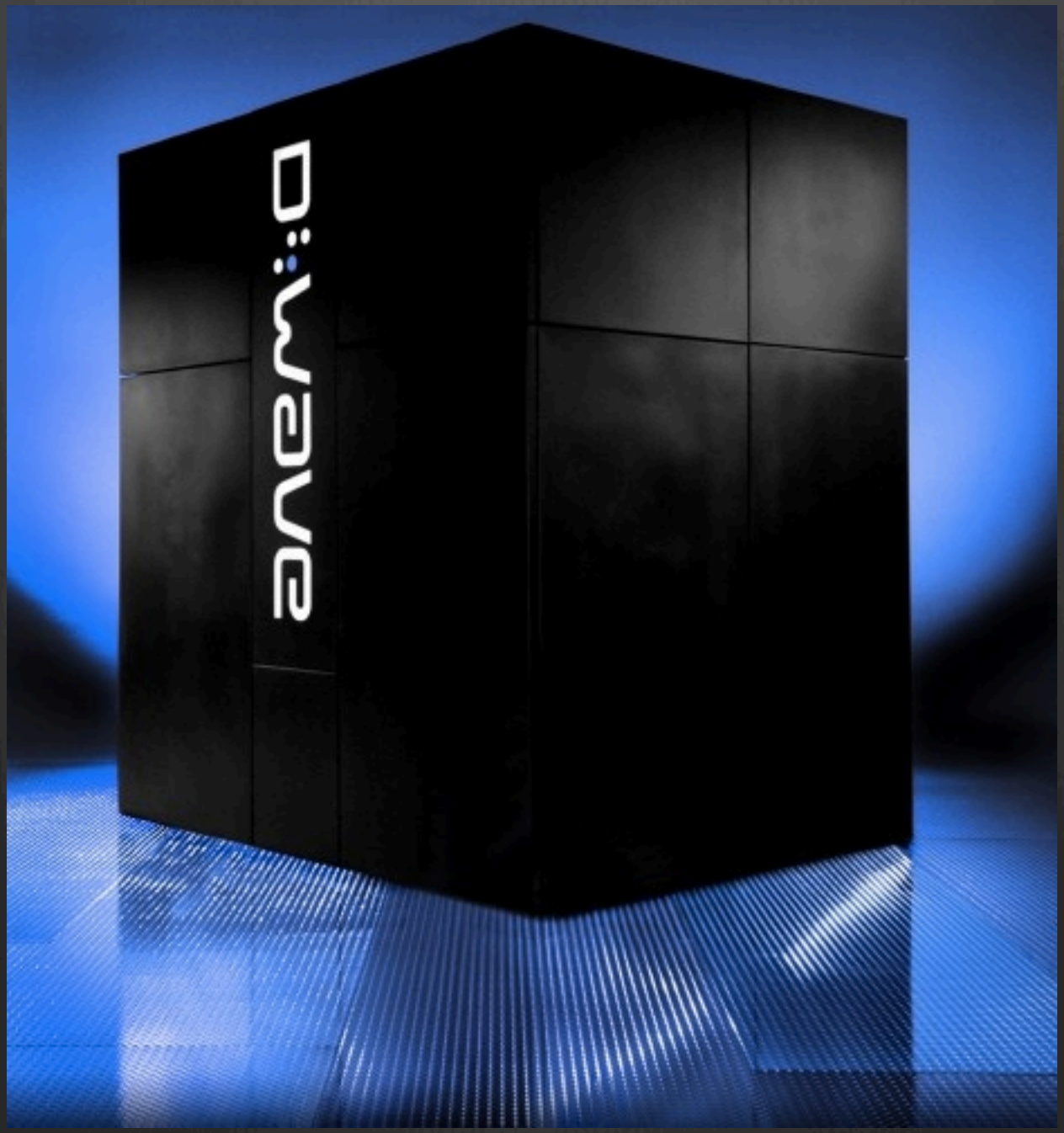
D::wave

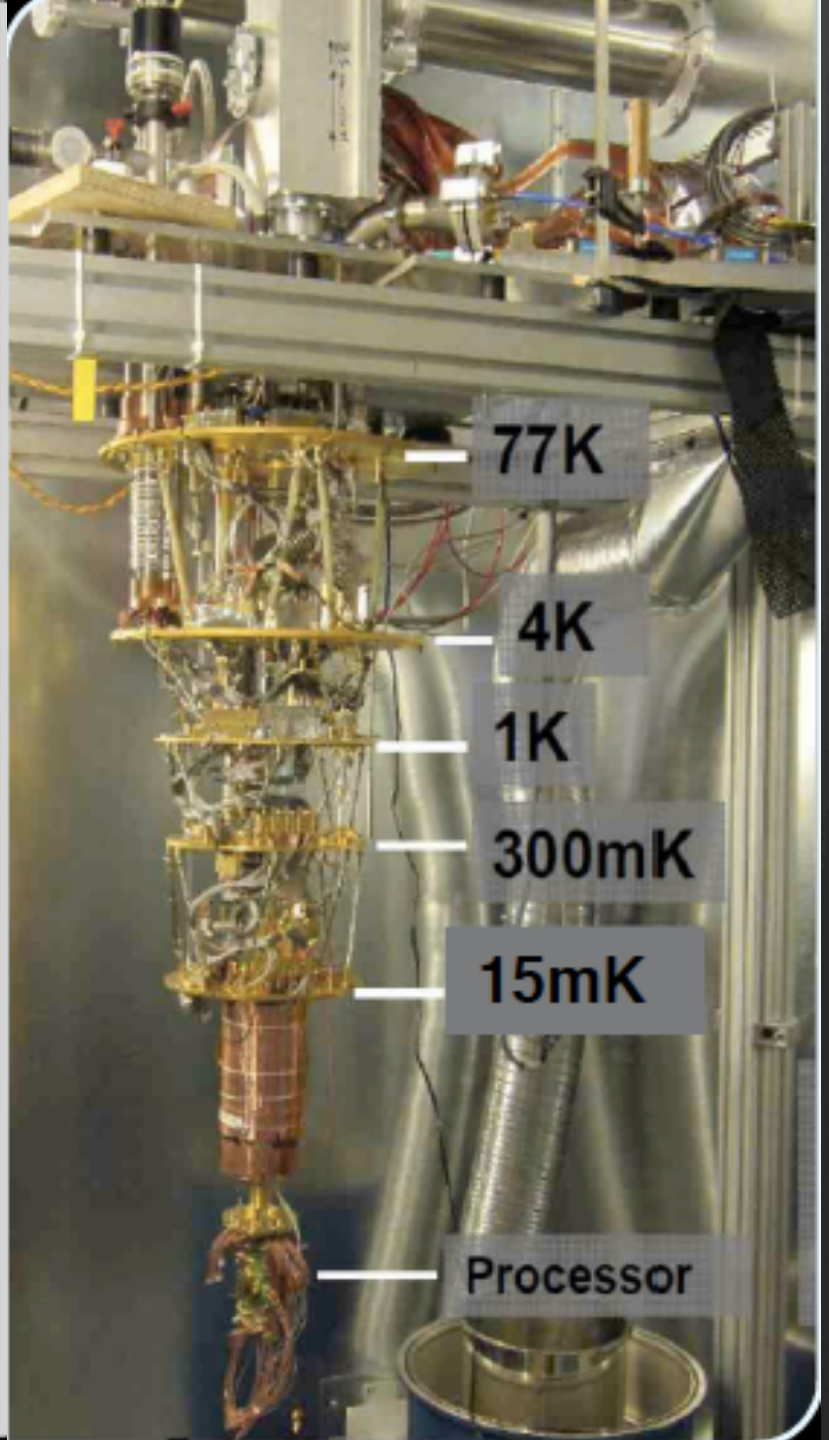
77K
4K
1K
300mK
15mK
Processor

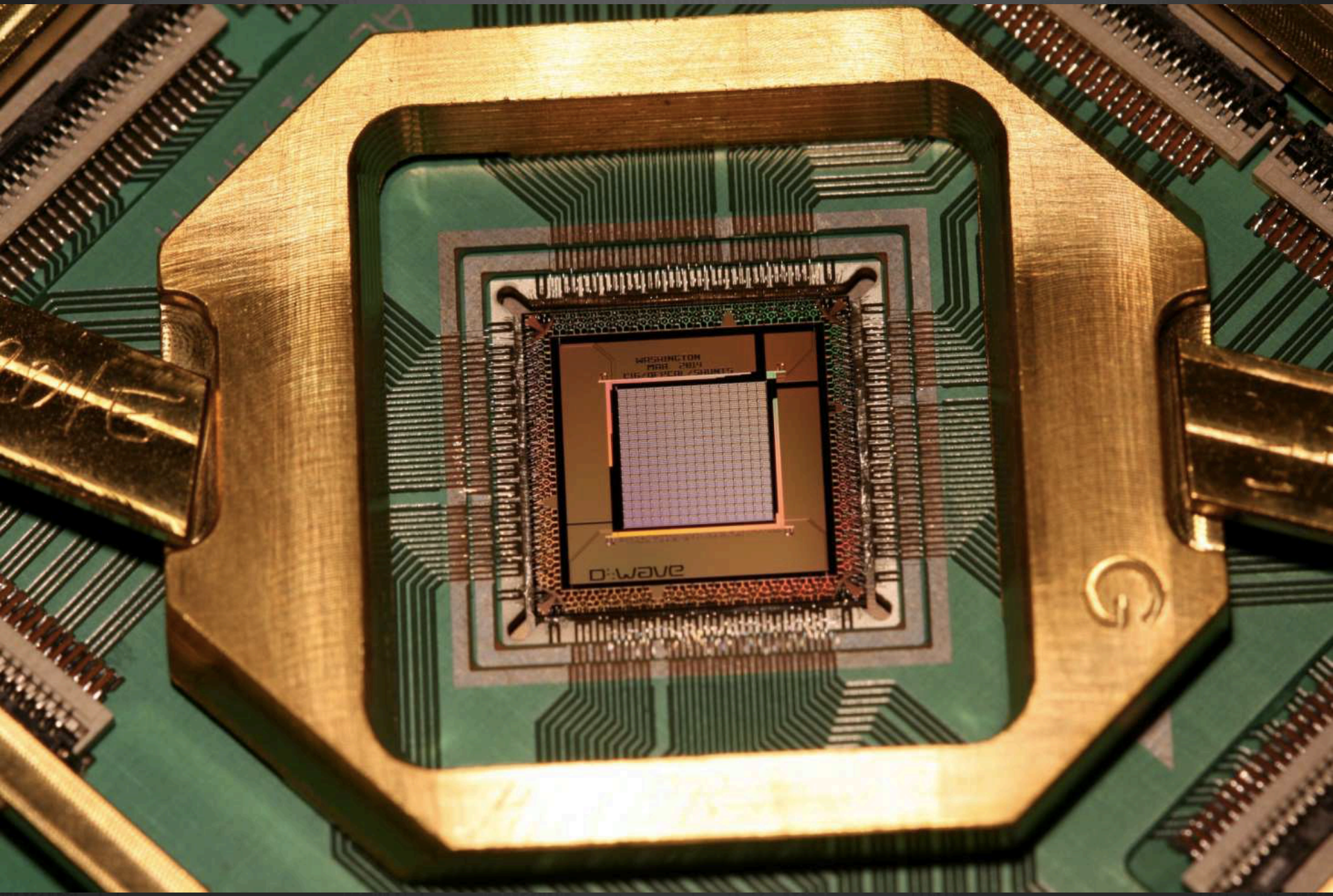
D-Wave

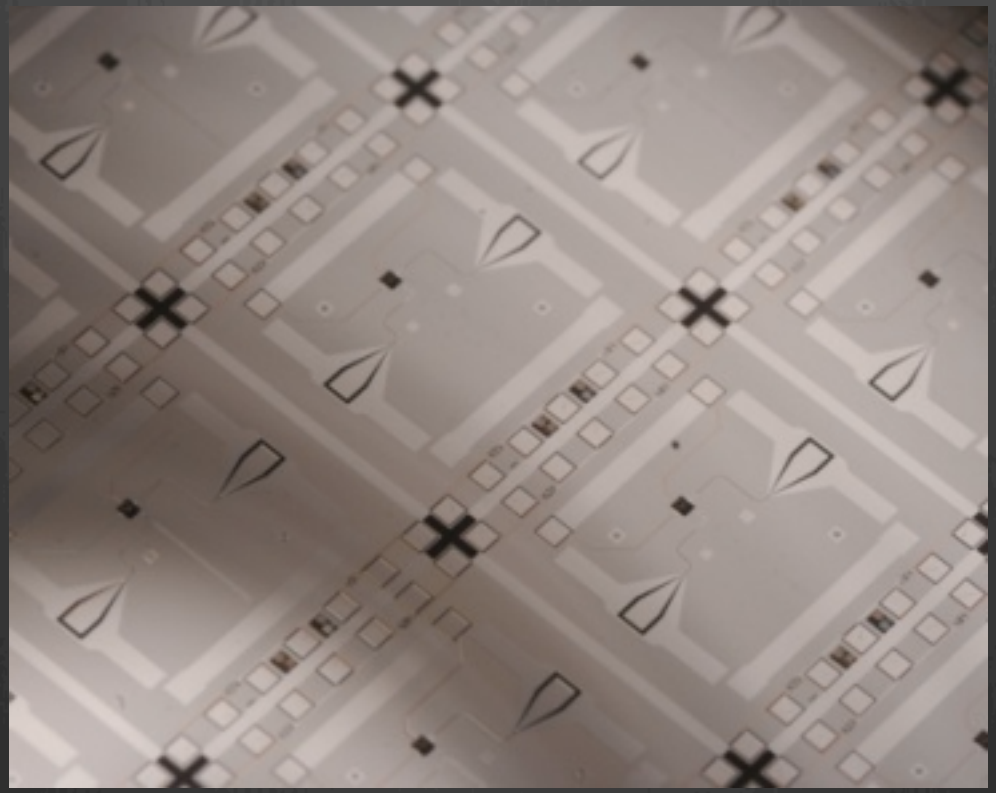

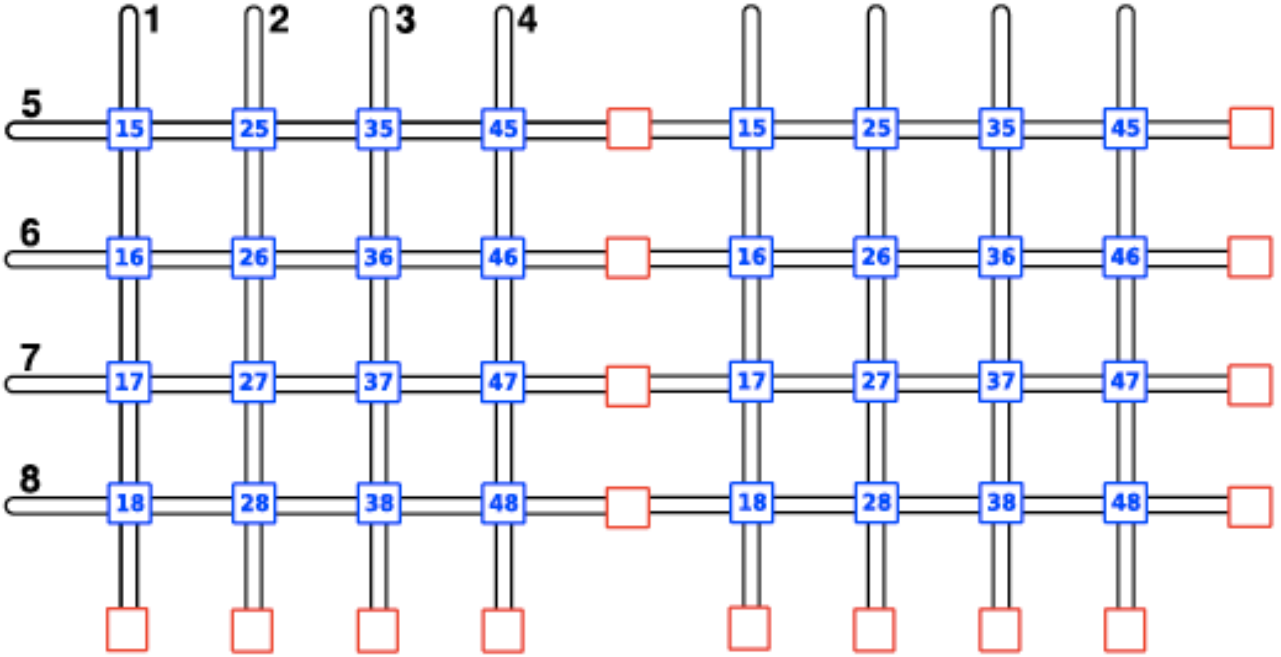
1
2
3
4
5
6
7
8
15
25
35
45
16
26
36
46
17
27
37
47
18
28
38
48

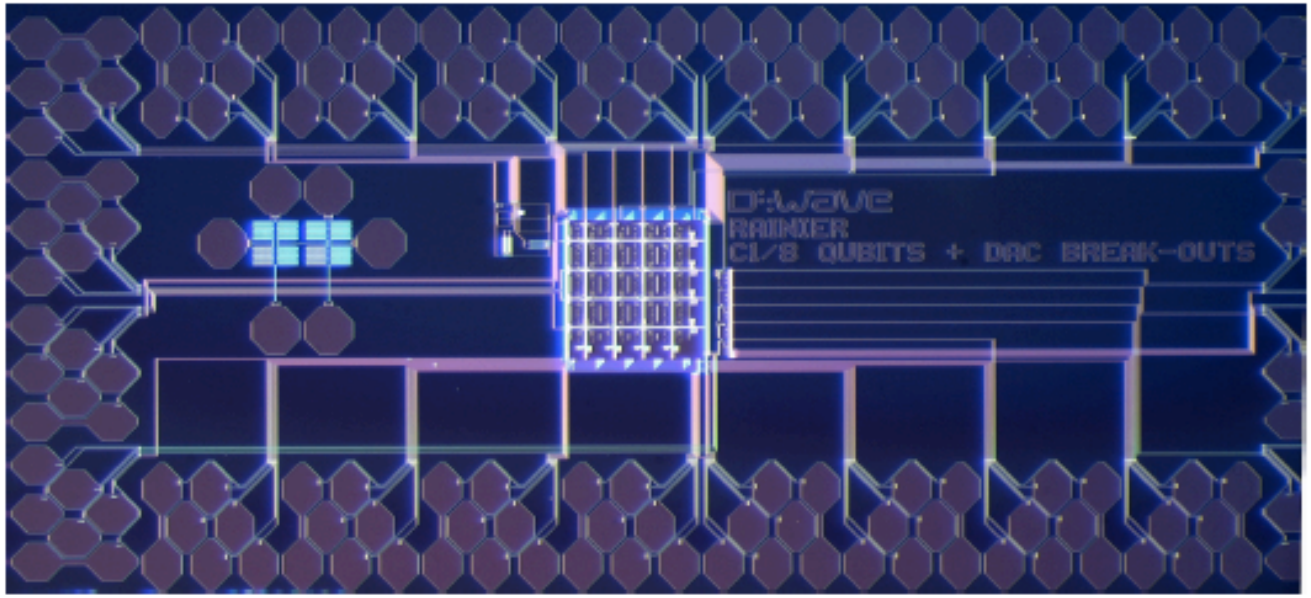
D-WAVE
RAINIER
C1/8 QUBITS + DAC BREAK-OUTS

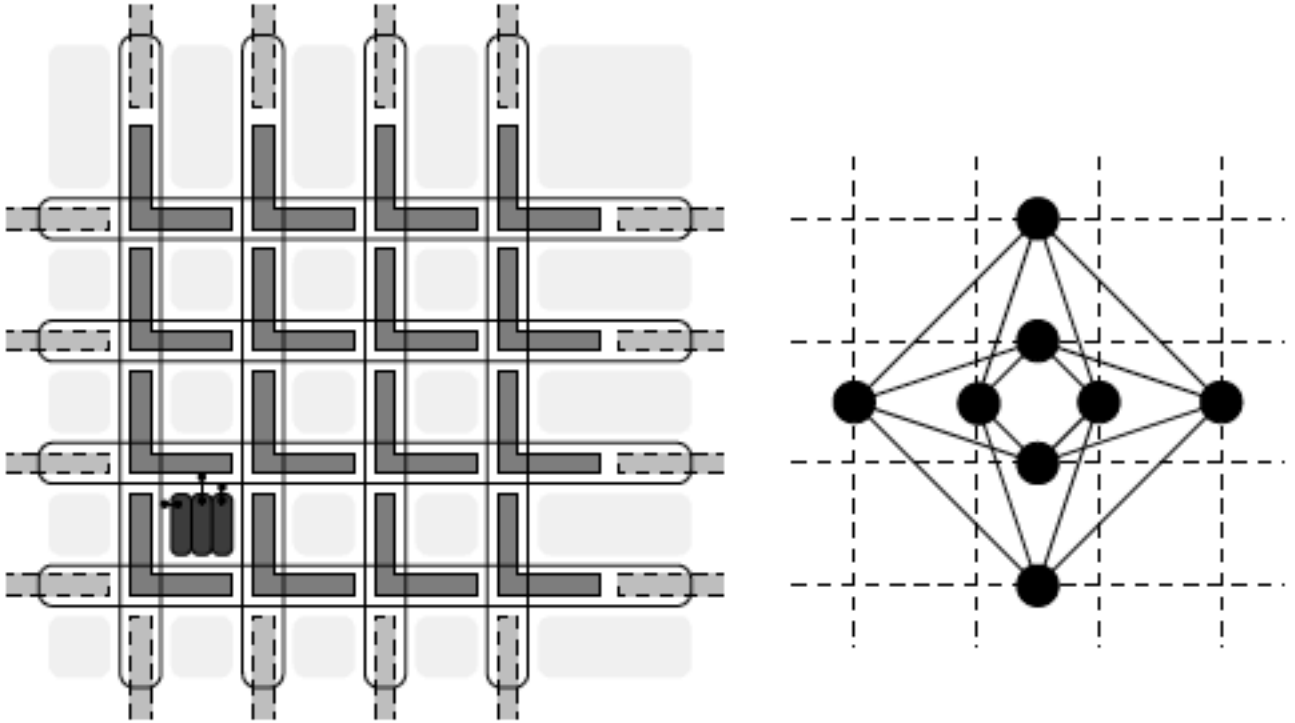

Fig. 1. Chimera unit cell topology. (Left) Layout sketch: qubit bodies are represented by the elongated loops that span the whole width/height of the unit tile. Each qubit is coupled to four others within the unit tile via the *internal coupler* bodies (dark L-shaped objects). Qubits are coupled to others in neighboring tiles via *external couplers* (lighter dashed rectangles). Control circuitry (Φ-DACs and corresponding analog control structures) are placed within light-shaded areas between the qubit/coupler bodies. (Right) Graph representation: each unit tile corresponds to a complete bipartite graph $K_{4,4}$ (dark nodes and solid line edges). Qubits from different tiles are coupled in square grid fashion (dashed edges).

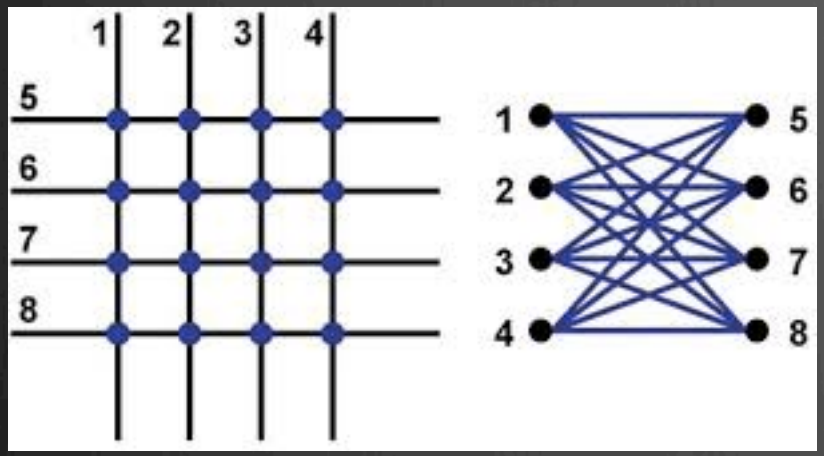
1
2
3
4
5
6
7
8
1
2
3
4
5
6
7
8

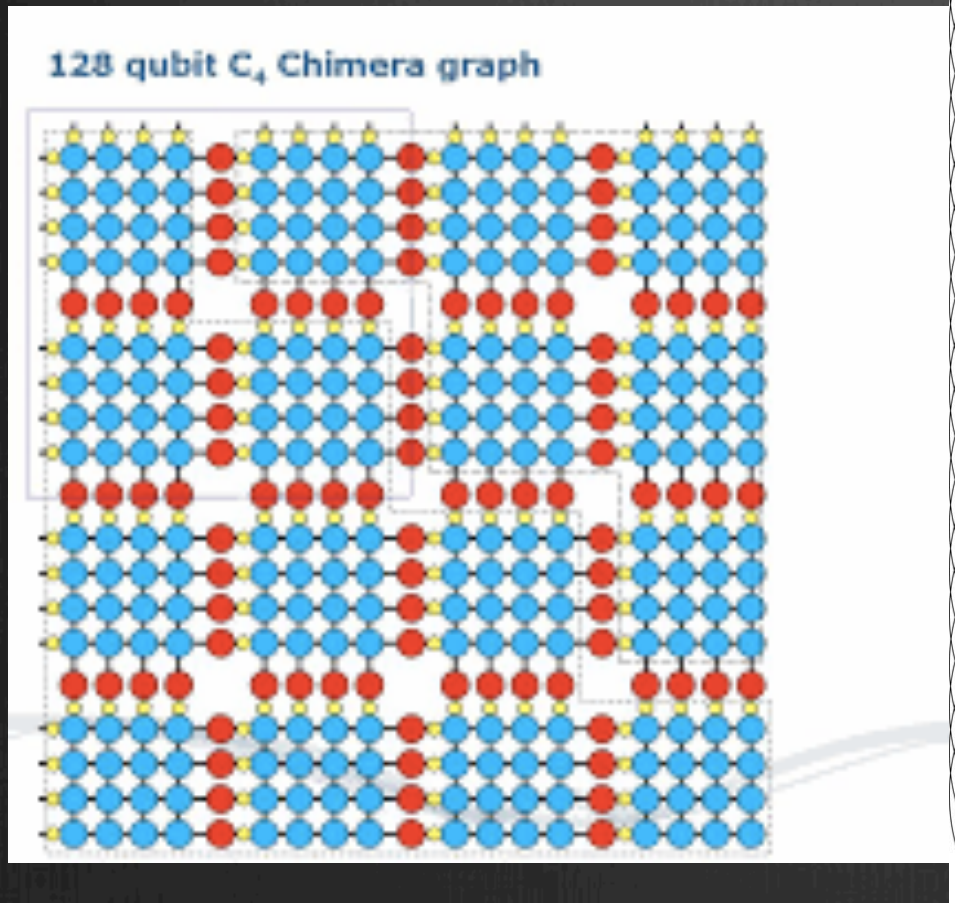
128 qubit C_4 Chimera graph

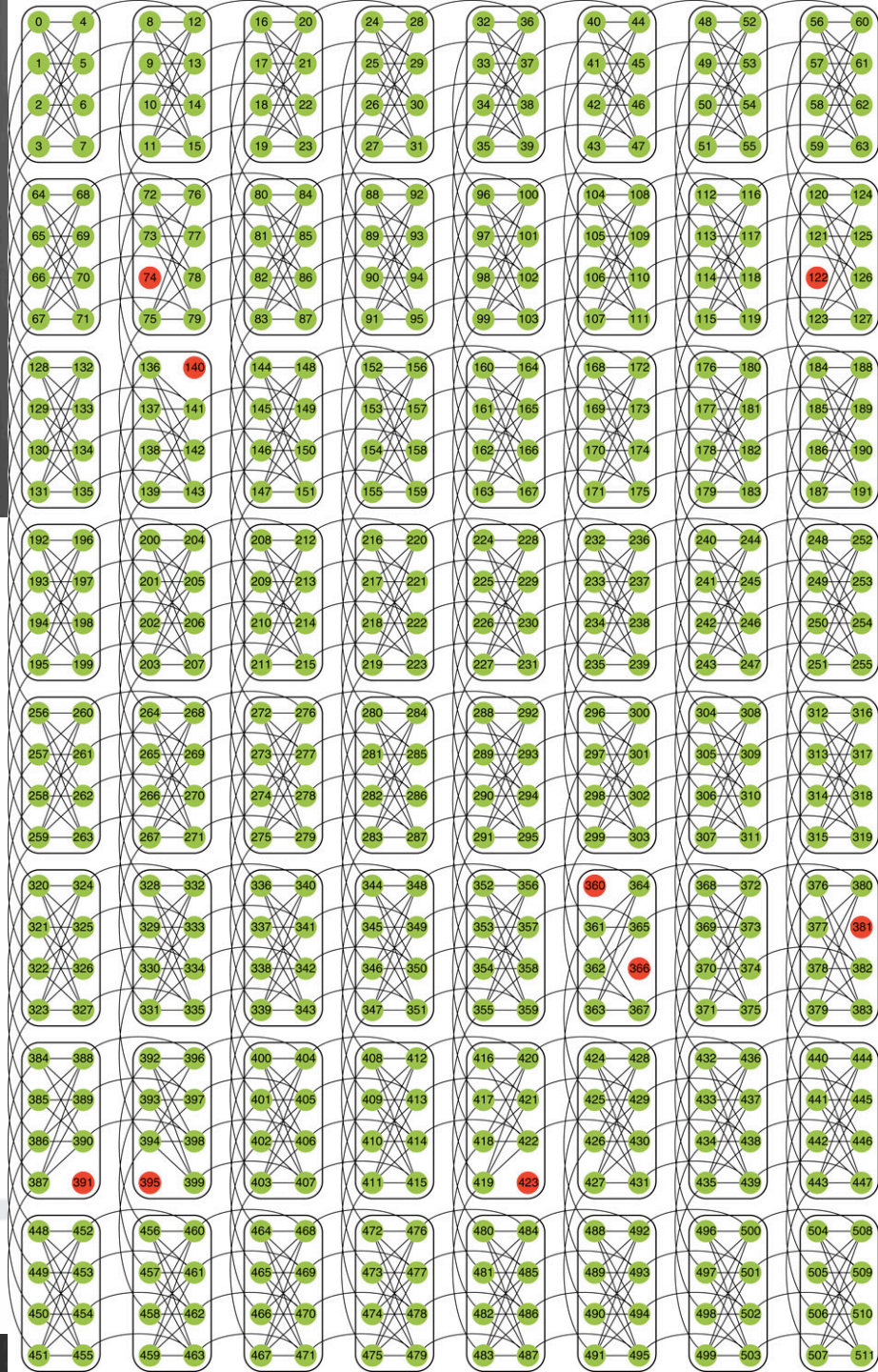

Programming D-Wave

Map coloring problem

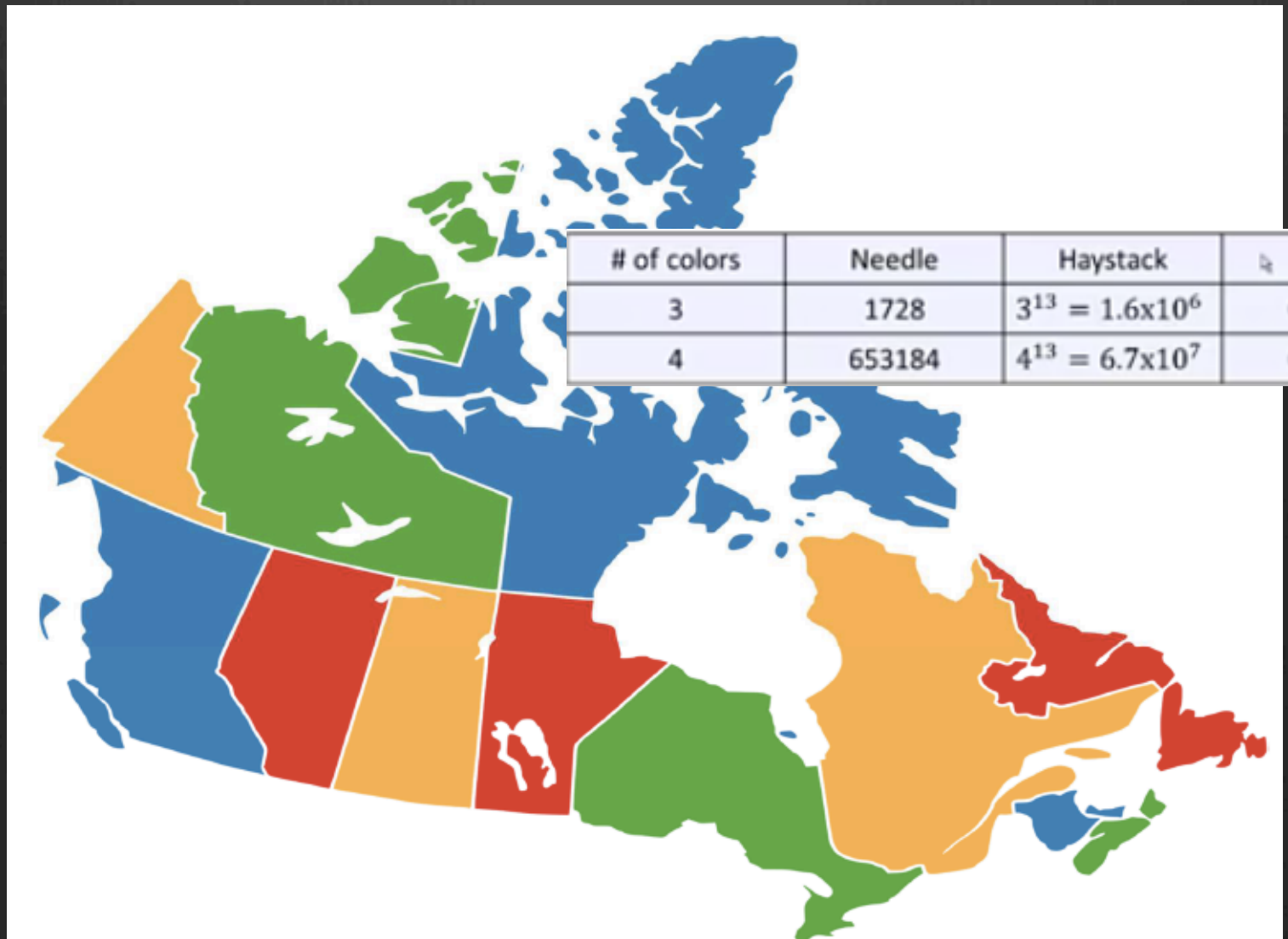

# of colors	Needle	Haystack	N/H
3	1728	$3^{13} = 1.6\text{x}10^{6}$	0.0011
4	653184	$4^{13} = 6.7\text{x}10^{7}$	0.0097

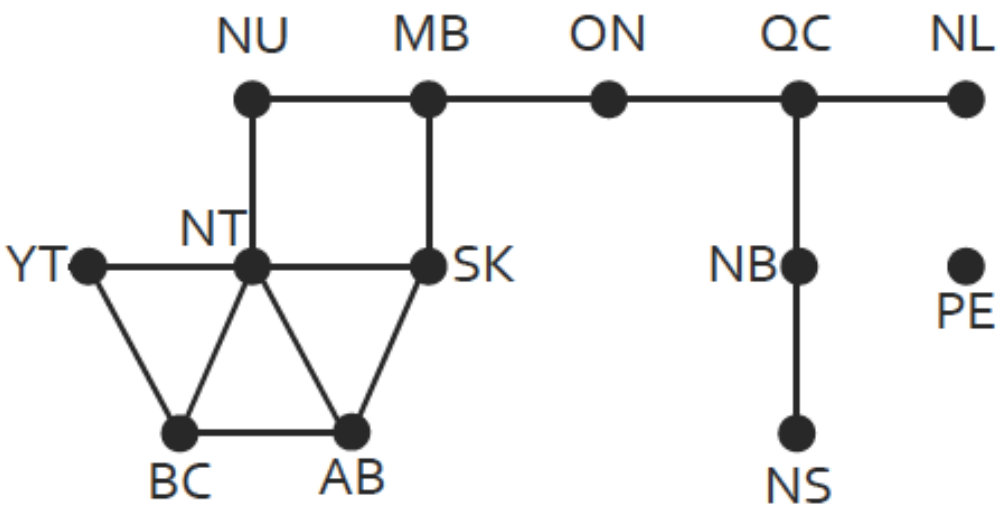

AB Alberta
BC British Columbia
MB Manitoba
NB New Brunswick
NL Newfoundland and Labrador
NS Nova Scotia
NT Northwest Territories
NU Nunavut
ON Ontario
PE Prince Edward Island
QC Quebec
SK Saskatchewan
YT Yukon

$$H = A\sum_{v}\left(1-\sum_{i=1}^{n}x_{v,i}\right)^{2} + A\sum_{(uv)\in E}\sum_{i=1}^{n}x_{u,i}x_{v,i}.$$

Objectives

$$O(\mathbf{a}, \mathbf{b}; \mathbf{q}) = \sum_{i=1}^{N} a_i q_i + \sum_{<i,j>} b_{ij} q_i q_j$$

q_1	q_2	$O(\mathbf{a}, \mathbf{b}; \mathbf{q})$
0	0	0
0	1	a_2
1	0	a_1
1	1	$a_1 + a_2 + b_{12}$

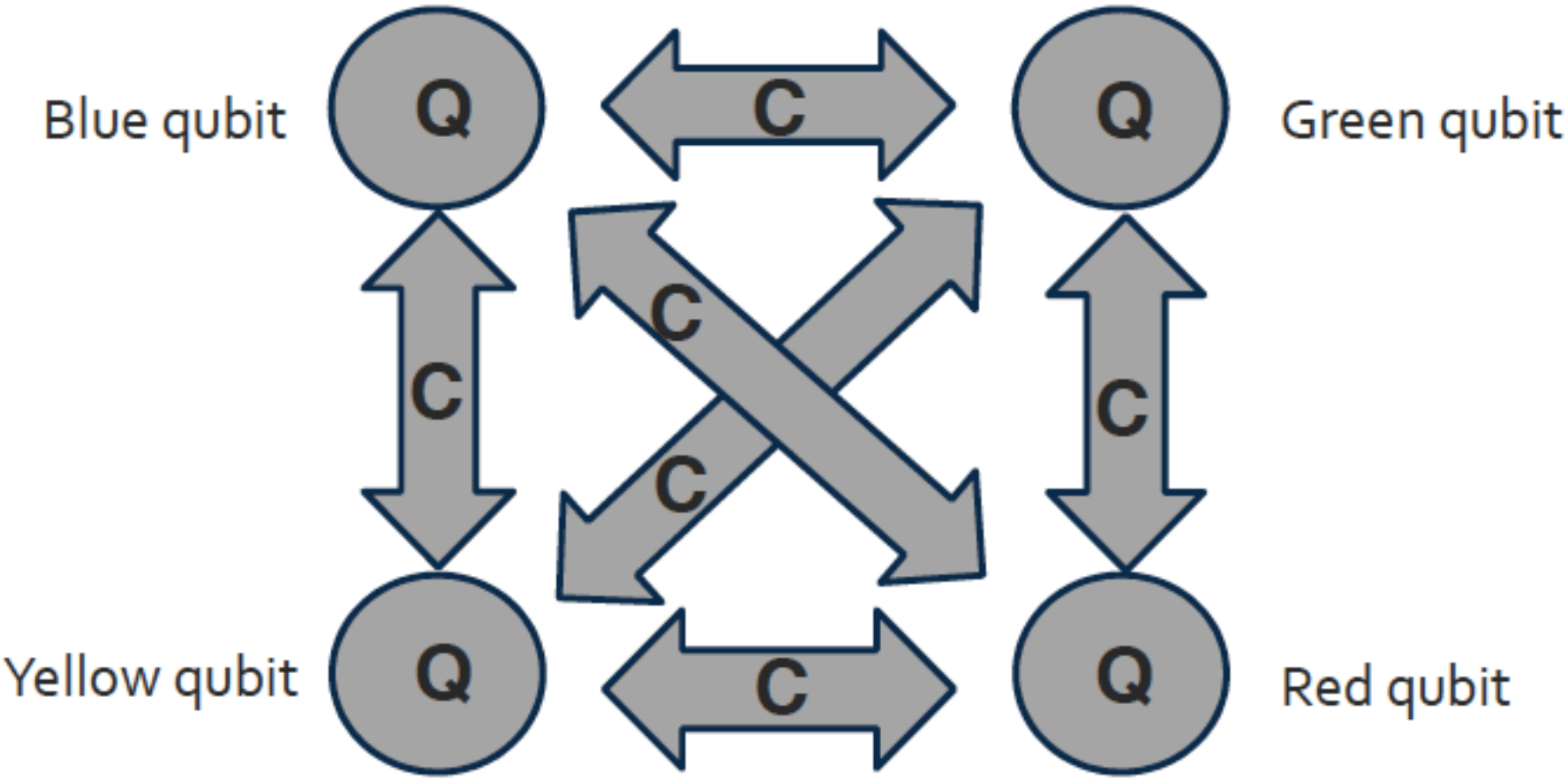

Objective : $O(q_b, q_g, q_r, q_y) = (q_b + q_g + q_r + q_y - 1)^2 \cong$

$$-1(q_b + q_g + q_r + q_y)$$

$$+2(q_b q_g + q_b q_r + q_b q_y + q_g q_r + q_g q_y + q_r q_y)$$

Maping onto the unit cell

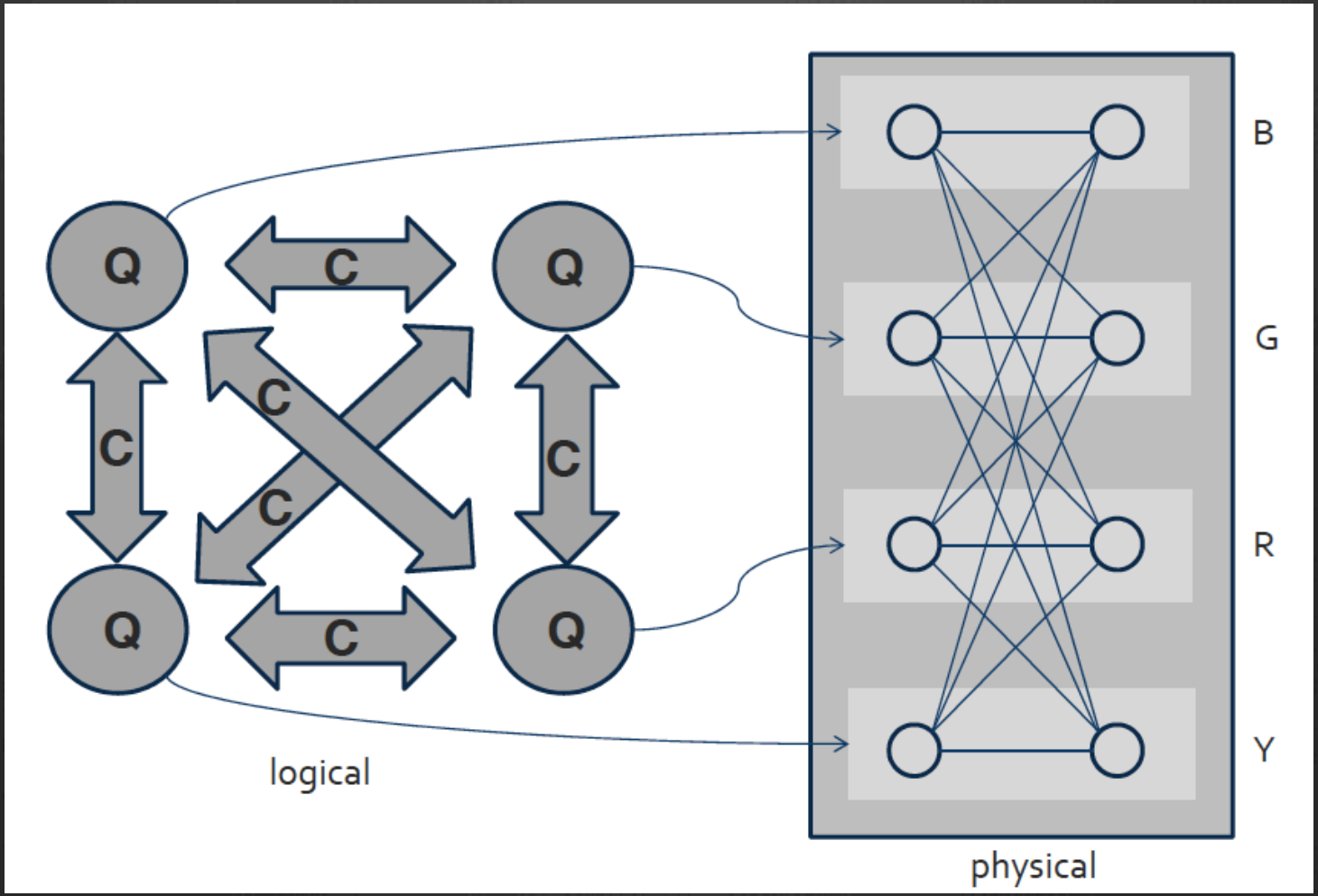

Code

```
/* STEP 1: turn on one of C qubits */
/* Handle weights                  */
for (i=0; i<C; ++i)
  {
    weight[DW_QUBIT(row,col,'L',i)] += -0.5;
    weight[DW_QUBIT(row,col,'R',i)] += -0.5;
  }
/* Handle strengths */
for (i=0; i<C; ++i)
  for (j=0; j<C; ++j)
    if (i != j)
      strength[DW_INTRACELL_COUPLER(row,col,i,j)] += 1;
```

Neighbors and cloning

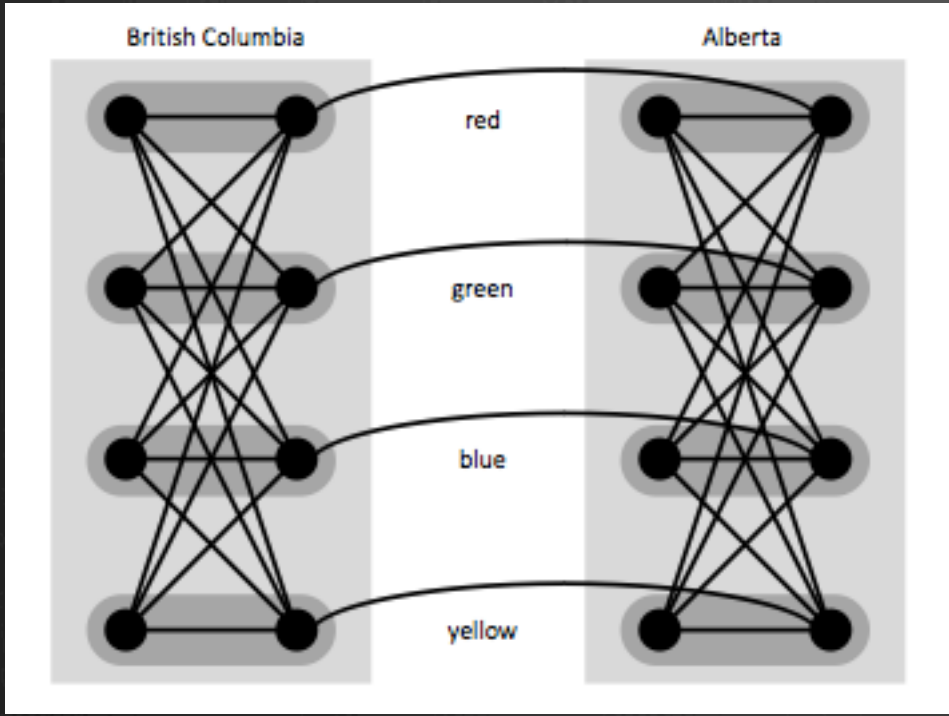

	0	1	2	3	4
0	NL	ON	MB	SK	AB
1	PE	QC	NU	NT	AB
2		NB	NS	NT	BC
3				YT	BC

GUI

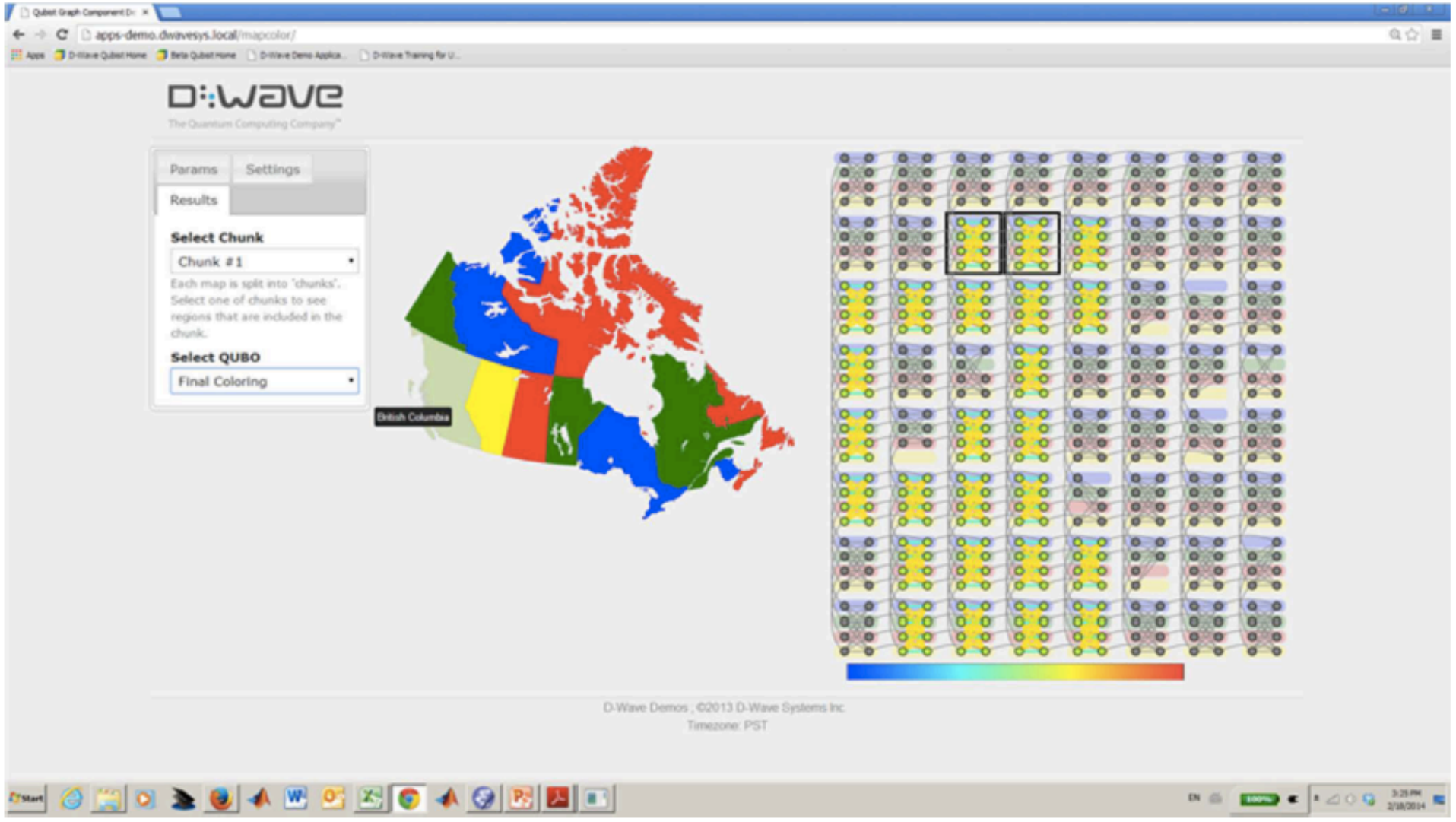
apps-demo.dwavesys.local/mapcolor/
D:Wave
The Quantum Computing Company™
Params
Settings
Results
Select Chunk
Chunk #1
Each map is split into 'chunks'. Select one of chunks to see regions that are included in the chunk.
Select QUBO
Final Coloring
British Columbia
D-Wave Demos , ©2013 D-Wave Systems Inc.
Timezone: PST

Chunks

Divide the US map into chunks.

Process the first chunk and get valid colorings for the first chunk of states.

Use these colorings to *bias* the second chunk.

Repeat.

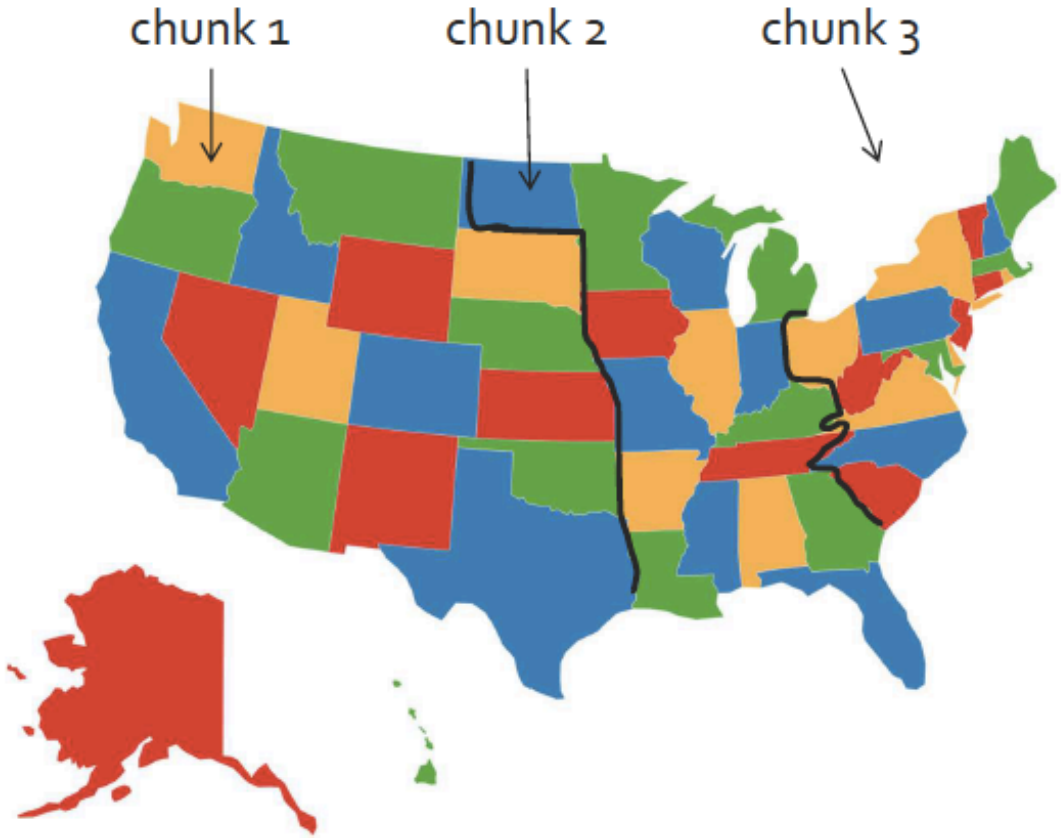

# of colors	Needle	Haystack	N/H
3	0	$3^{49} = 2.4\text{x}10^{23}$	0
4	25623183458304	$4^{49} = 3.2\text{x}10^{29}$	$8\text{x}10^{-17}$

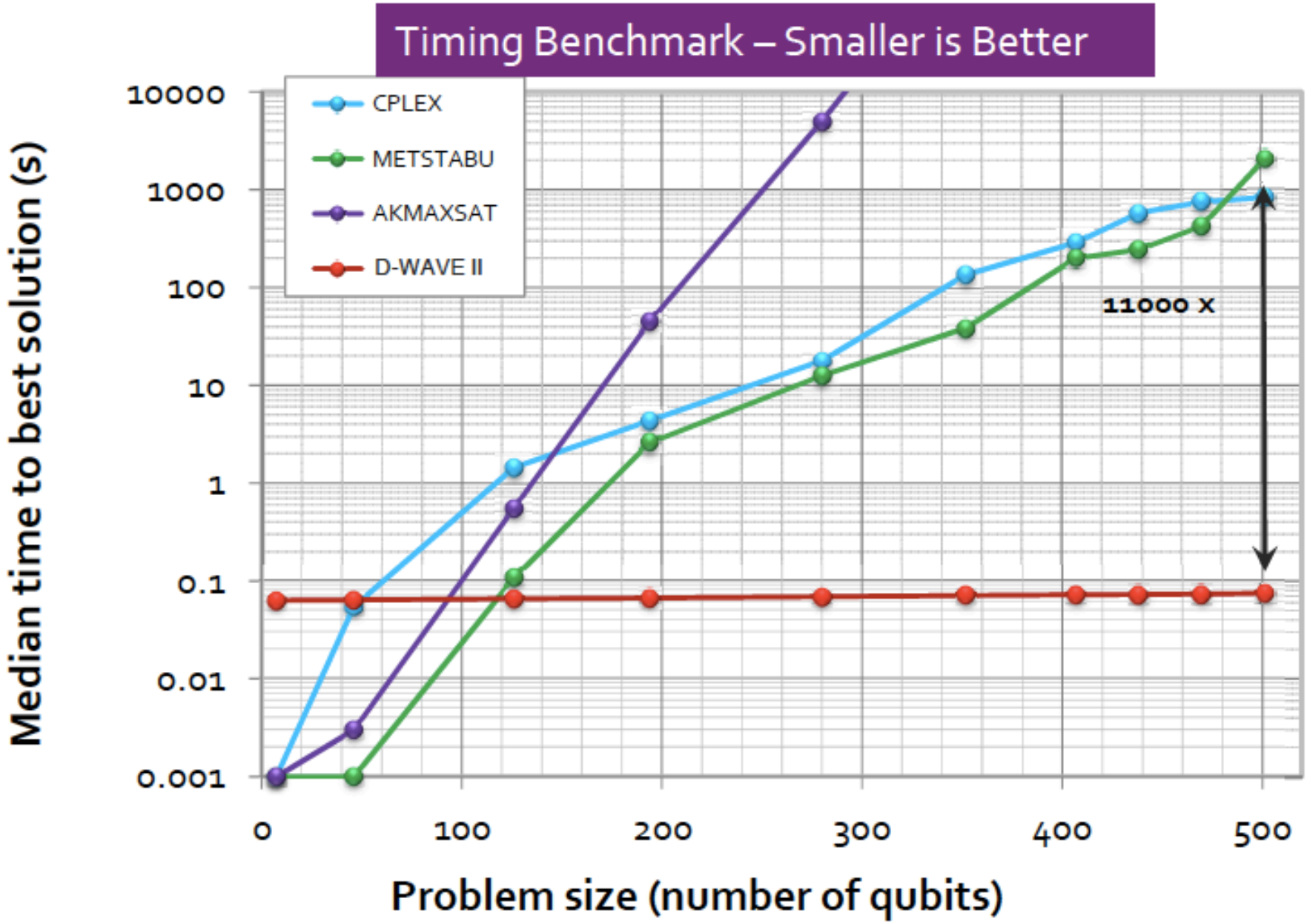
Timing Benchmark – Smaller is Better
CPLEX
METSTABU
AKMAXSAT
D-WAVE II
11000 X
10000
1000
100
10
1
0.1
0.01
0.001
0
100
200
300
400
500
Median time to best solution (s)
Problem size (number of qubits)

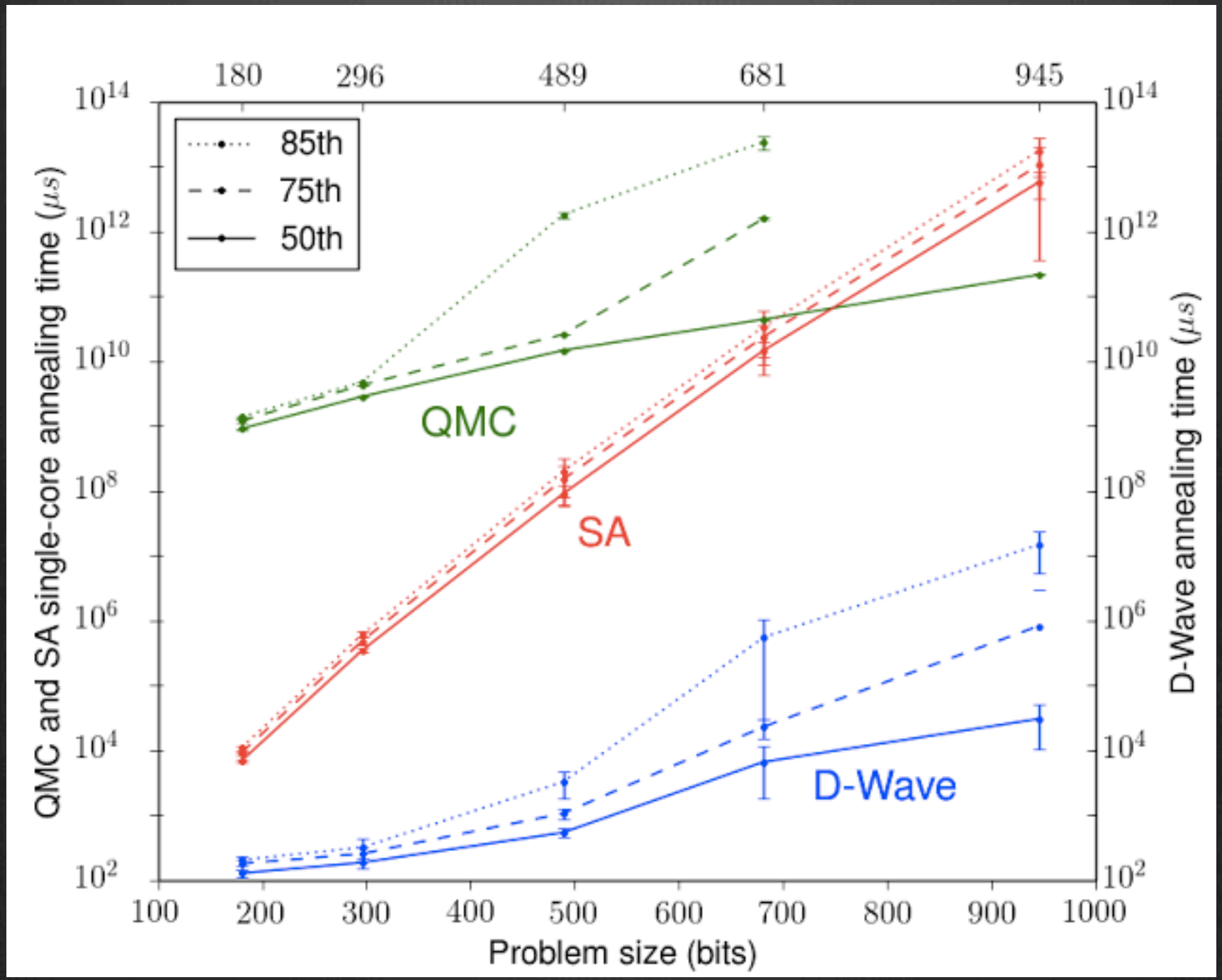
180
296
489
681
945
85th
75th
50th
QMC
SA
D-Wave
QMC and SA single-core annealing time (μs)
D-Wave annealing time (μs)
Problem size (bits)
10^{14}
10^{12}
10^{10}
10^{8}
10^{6}
10^{4}
10^{2}
100
200
300
400
500
600
700
800
900
1000

Machine Learning: Binary Classification

- Traditional algorithm recognized car about 84% of the time
- Google/D-Wave Qboost algorithm implemented to recognize a car (cars have big shadows!)
- "Quantum Classifier" was more accurate (94%) and more efficient
- Ported quantum classifier back to traditional computer, more accurate and fewer CPU cycles (less power)!

D-Wave
The Quantum Computing Company™

© 2016 D-Wave Systems Inc. All Rights Reserved

Outlook

THE JOURNAL OF CHEMICAL PHYSICS **134**, 174504 (2011)

Exciton dynamics in chromophore aggregates with correlated environment fluctuations

Darius Abramavicius[1,a)] and Shaul Mukamel[2,b)]
[1]*State Key Laboratory of Supramolecular Structure and Materials, Jilin University, People's Republic of China, and Physics Faculty, Vilnius University, Lithuania*
[2]*Chemistry Department, University of California Irvine, California 92697-2025, USA*

(Received 18 February 2011; accepted 27 March 2011; published online 5 May 2011)

We study the effects of correlated molecular transition energy fluctuations in molecular aggregates on the density matrix dynamics, and their signatures in the optical response. Correlated fluctuations do not affect single-exciton dynamics and can be described as a nonlocal contribution to the spectral broadening, which appears as a multiplicative factor in the time-domain response function. Intraband coherences are damped only by uncorrelated transition energy fluctuations. The signal can then be expressed as a spectral convolution of a local contribution of the uncorrelated fluctuations and the nonlocal contribution of the correlated fluctuations. © *2011 American Institute of Physics*.
[doi:10.1063/1.3579455]

number of excitons. The chromophores are electrically
tral and interact via the dipole–dipole Coulomb interacti
The electronic charge densities of different chromophore
not overlap so that electron exchange is negligible. In
molecular basis set the Frenkel exciton Hamiltonian read

$$\hat{H}_S = \sum_m \varepsilon_m \hat{B}_m^\dagger \hat{B}_m + \sum_{m,n}^{m\neq n} J_{mn} \hat{B}_m^\dagger \hat{B}_n,$$

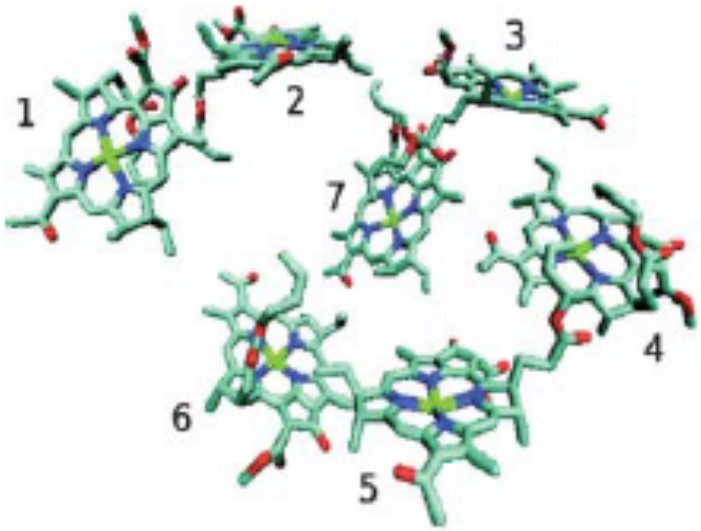

FMO as a little quantum computer

"When viewed in this way, the system is essentially performing a single quantum computation, sensing many states simultaneously and selecting the correct answer, as indicated by the efficiency of the energy transfer. In the presence of quantum coherence transfer, such an operation is analogous to Grover's algorithm, with the hamiltonian describing both relaxation to the lowest energy state and coherence transfer (refilling the coherence lost from the transfer to the lowest-energy state); such a scheme can provide efficiency beyond that of a classical search algorithm. This mechanism contrasts with a semiclassical 'hopping' mechanism through which the excitation moves stepwise from exciton state to exciton state, dissipating energy at each step, which would be similar to a classical search where only one state can be occupied at any one time. Such a mechanism also raises the possibility of non-local events, although more detailed analysis is needed before we can determine whether such effects are present in FMO."

Fleming and Engel (Nature, 2007)

FMO is searching the energy minimum

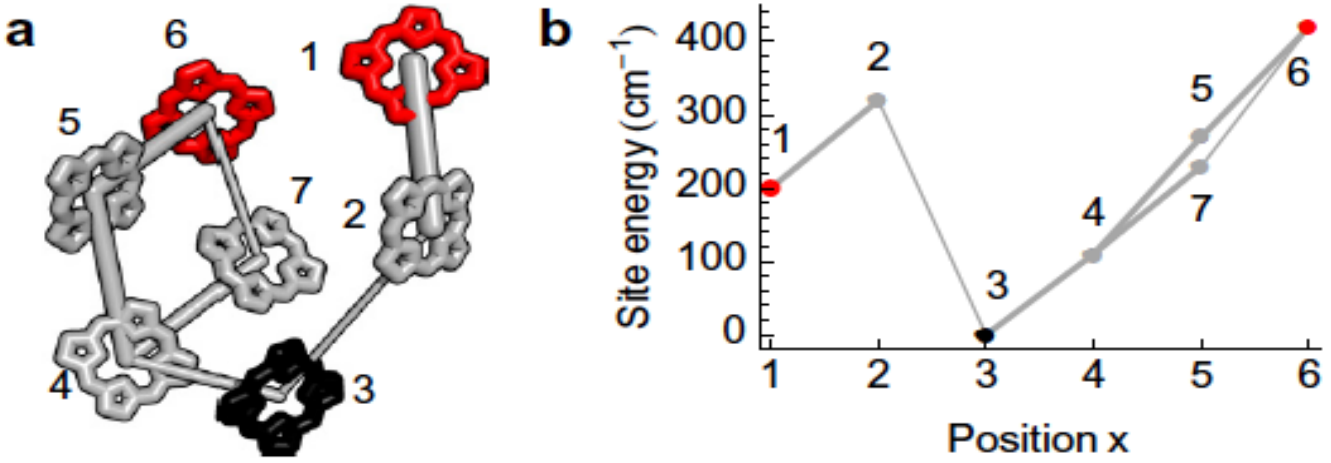

Figure 1. (a) Crystal structure of the FMO complex of *C. tepidum* (Protein Data Bank accession 3ENI), with lines between the chromophores representing dipolar couplings. The thickness of the lines indicates the coupling strengths. Only couplings above 15 cm^{-1} are shown; the largest coupling is 96 cm^{-1}. The full Hamiltonian is given in appendix A. (b) Site energies, shown relative to 12 210 cm^{-1}, in the reduced dimensionality model derived from mapping the strongest couplings onto a one-dimensional graph. The red sites (1, 6) are source sites at which the excitation enters the complex and the black site (3) is the trap site from which the excitation is transferred to the reaction center [27, 28].


Not Magic...
QUANTUM